Journal of Thermal Engineering
https://jten.yildiz.edu.tr/
https://doi.org/10.47481/jten.0073

RESEARCH ARTICLE

Hydrothermal performance of triple periodic boundary conditions; oscillatory flow, wavy surfaces, and fluctuating heat flux: a review

Zina M. Salih[1], Saad M. Jalil[2,*]

[1]Department of Mechanical Engineering, Engineering College, University of Anbar, 31001, Iraq
[2]Department of Mechanical Engineering, Engineering College, University of Anbar, 31001, Iraq

Abstract

Enhancing heat transfer while minimizing pressure drop is a critical challenge in compact heat exchanger design. This review examines oscillatory flow and periodic surface geometries as promising solutions because they play a significant role in disrupting boundary layers, promoting mixing, and enhancing convective performance. Analytical, numerical, and experimental methods for sinusoidal and corrugated channels under both uniform and non-uniform heat fluxes are systematically reviewed. Most previous reviews have addressed oscillatory or steady flows in smooth or wavy tubes under uniform heat flux, while the combined influence of oscillatory flow, wavy geometry, and time-varying heat flux remains largely unexplored. This review highlights a gap by analysing available studies on hybrid thermal–hydrodynamic interactions from 2005 to 2025. The most significant finding was that periodic geometries can enhance heat transfer by up to four- to fivefold compared with smooth channels. Compared with non-oscillatory flow at the same Reynolds number, the Nusselt number increases by up to 20%. This improvement is primarily due to oscillatory motion, which disrupts the thermal boundary layer and enhances fluid mixing, thereby intensifying convective heat transfer. It can be concluded from these results that a hybrid strategy combining periodic surfaces and oscillatory flow can achieve significant enhancement of heat transfer while maintaining controllable pressure losses. Beyond previous studies that addressed active (oscillation) and passive (geometry) methods independently, this work introduces a new consideration of triple-periodic boundary conditions by integrating the oscillatory flow and the wavy surface under an actual unsteady heat flux. Knowledge gained from this review can be immediately applied to a wide range of real-world systems where effective thermal management is crucial.

Keywords: Oscillatory flow, wavy surface, periodic, fluctuating heat flux, heat exchanger

Cite this article as: Salih, Z. M., & Jalil, S. M. (2026). Hydrothermal performance of triple periodic boundary conditions; oscillatory flow, wavy surfaces, and fluctuating heat flux: A review. Journal of Thermal Engineering, 12(5), 1886–1914. https://doi.org/10.47481/jten.0073

1. Introduction

A crucial component of thermal systems is the heat exchanger, which transfers heat across a solid boundary separating two or more fluids. The conclusions of the current review are directly applicable to various real-world applications in which accurate thermal management is crucial, such as regenerative cooling systems, oscillating heat pipes, thermoacoustic engines, and compact heat exchangers. All of these require efficient heat management techniques to operate reliably. A possible method is to incorporate periodic surfaces into the heat exchanger channels, which disrupt the boundary layer and promote flow mixing, thereby increasing the effective heat transfer area. These periodic components, such as wavy walls, ribs, and corrugations, enhance convective heat transfer. In parallel with the development of geometrical modifications, oscillatory flow has introduced an innovative method to enhance thermal performance [1]. When paired with periodic surfaces that naturally disrupt the flow, this unstable flow regime enhances mixing, continuously renews the boundary layer, and improves heat transfer rates. The combination of oscillatory flow with periodic surfaces results in a complex and rich fluid-thermal interface. Periodic surfaces enhance local heat transfer by inducing geometric turbulence, while oscillatory flow introduces additional periodic disturbances, resulting in complex secondary flows, thermal gradients, and vortices. The thermal and hydrodynamic properties of oscillatory flow in periodic surface heat exchangers remain poorly understood,

*Corresponding Author
E-mail Adress: saad.jalil@uoanbar.edu.iq

Submitted: 25 July 2025; **Accepted:** 17 November 2025

This paper was recommended for publication in revised form by Editor-in-Chief Ahmet Selim Dalkılıç

despite their potential advantages. Numerous factors, including surface geometry, flow regime (laminar or turbulent), oscillation frequency, and amplitude, interact nonlinearly, necessitating in-depth analytical, computational, and experimental studies.

The current review will focus on the most recent research, examine how the main parameters are affected by periodic behaviour, and specify the availability of further analyses to address gaps in this field. Triply periodic or fluctuating boundary conditions can shift thermal improvement methods to focus not only on conventional geometrical modifications but also on other factors. Therefore, even though oscillatory flows and periodic surface geometries have been widely studied, earlier reviews have mostly treated these two approaches independently and often under simplified uniform heating conditions. However, the hybrid interactions between oscillatory motion and wall periodicity under non-uniform or transient heat fluxes remain largely unexplored. Hence, it leaves a shortcoming in the understanding of their hybrid effects, particularly under non-uniform heat flux, which is more representative of real applications. The originality of the this review lies in its systematic integration of analytical, numerical, and experimental studies, providing a unified perspective on how oscillatory (active) and periodic (passive) techniques complement each other, particularly in the context of transient heat flux. Therefore, this work presents a new framework that surpasses earlier surveys and serves as a guide for both fundamental research and engineering design.

2. Main characterized parameters

In the context of oscillatory flow in periodic surface heat exchangers, essential geometric parameters and flow characteristics have a significant impact on the heat transfer rate and pressure drop. Some of these crucial parameters are listed below:

2.1. Performance evaluation criterion

The Performance Evaluation Criterion(PEC) in heat transfer is a dimensionless parameter used to measure the thermal-hydraulic performance of a heat exchanger or a flow system. It quantifies the trade-off between heat transfer enhancement and the associated pressure drop effect [2] as a ratio between the enhanced value and the reference value. The PEC is typically expressed as:

$$\mathrm{PEC} = \frac{\left(\frac{\mathrm{Nu_{enh}}}{\mathrm{Nu_{ref}}}\right)}{\left(\frac{\mathrm{f_{enh}}}{\mathrm{f_{ref}}}\right)^{\frac{1}{3}}} \quad (1)$$

Where Nu_{ref} and f_{ref} are the Nusselt number and the friction factor for the reference (smooth) tube, and Nu_{enh}. and f_{enh} are the Nusselt number and the friction factor for the enhanced(wavy)tube. All terms in Eq.(1)are dimensionless, ensuring dimensional consistency.

2.2. Wavelength (pitch)

The pitch refers to the distance between periodic structures in the heat exchanger. It is typically measured in the direction of flow. In heat exchangers with corrugated, wavy, or finned surfaces, the pitch is the distance between successive peaks. This parameter plays a significant role in both fluid flow and heat transfer behaviour. A smaller pitch increases the surface area, causing greater turbulence in the fluid, which improves heat transfer performance but increases pressure drop. On the other hand, a larger pitch reduces the pressure drop by allowing smoother flow, which lowers heat transfer efficiency due to reduced surface interaction and mixing [3].

2.3. Wave amplitude

The amplitude is the height of the periodic surface feature above its baseline (or mid-plane) and represents how much a periodic structure deviates from a flat surface. On wavy or corrugated surfaces, the amplitude is half the vertical distance between the highest and lowest points in a single wavelength. The amplitude of the periodic surface geometry of a heat exchanger also plays a crucial role in determining heat transfer and flow behaviour. An increase in amplitude leads to greater flow disturbance and mixing, which enhances convective heat transfer by generating turbulence and increasing interaction between the surface and the fluid. Additionally, it introduces increased resistance to flow and the potential for flow separation, which can lead to a greater pressure drop. On the other hand, a lower amplitude leads to a more streamlined flow with less resistance and minimal pressure loss, but at the possible cost of reduced heat transfer performance due to decreased fluid agitation and surface interaction [3].

2.4. Oscillatory flow

Oscillatory flow is a type of unsteady flow that occurs when the fluid's velocity periodically changes with a back-and-forth motion within the flow region. Oscillatory flow is more complex than steady flow, which has a constant direction and velocity. Applying an external force as an active technique, such as mechanical pistons or imposed boundary conditions, results in cycles of acceleration and deceleration. This behaviour results in intricate relationships between inertia, viscosity, and thermal diffusion, which produce unique thermal and hydrodynamic properties, in contrast to those expected in steady flows. Oscillatory flow can be classified into two categories, depending on both temporal and spatial factors: pulsating and reciprocating flows. In addition to the flow characteristics and driving mechanism, as shown in Figure 1.

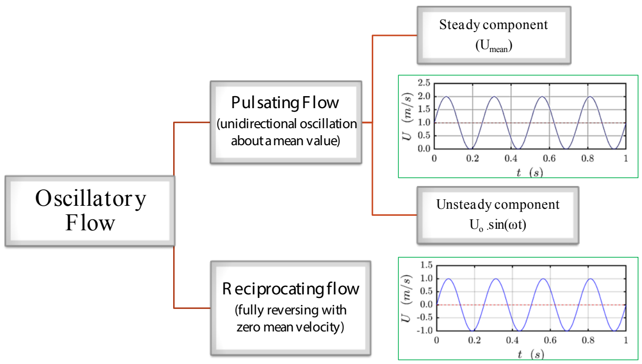

Figure 1. Oscillatory flow classification

The velocity of oscillatory (reciprocating) flow can be characterized by Eq. 2a, which describes a fully reversed flow with zero mean velocity. Pulsating flow, as defined in Eq. 2b, is with steady (U_{mean}) and unsteady velocity components under constant fluctuating amplitude (U_o)[4].

$$U(t) = U_o \sin(\omega t) \tag{2a}$$

$$U(t) = U_{mean} + U_o \sin^{\circ}(\omega t) \tag{2b}$$

Where U(t) is the instantaneous velocity (m/s), U_o is the oscillation amplitude (m/s), ω is the angular frequency of oscillation (rad/s), t is time (s), and U_{mean} is the mean (steady) velocity component (m/s). All terms in Eqs.(2a)and(2b)are dimensionally consistent, with velocity expressed in m/s.

Oscillatory flow plays a significant role in enhancing heat and momentum transfer in periodic geometric systems. Unlike steady flow, where heat transfer is reduced through the development of thermal and velocity boundary layers, oscillatory motion tends to continually disrupt and regenerate the boundary layer through periodic acceleration and flow reversal. The cyclic fluctuation of the boundary layer sustains high-temperature gradients near the surface, resulting in improved thermal performance. Additionally, when wavy surfaces are present, oscillations generate secondary flows in the form of localized vortices and recirculation zones, which enhance mixing between the core and wall fluids, thereby significantly improving convective heat transfer. Periodic acceleration also enhances thermal diffusion, especially when the oscillation parameters are comparable to the thermal response time, which can be characterized by dimensionless parameters such as the Womersley and Strouhal numbers. In addition, oscillatory flow offers control over residence time by adjusting frequency and amplitude, making it a valuable design option for optimizing the trade-off between heat transfer and pressure drop. At low Reynolds numbers, oscillations can also induce an early transition to turbulence, especially in channels with periodic characteristics, thereby enhancing convective heat transfer even at low bulk flow velocities. Table 1 lists the most critical parameters that control the oscillatory flow, such as the Stokes boundary layer and the dimensionless number that specifies the limitation of the oscillatory flow[5].

Table 1. Oscillatory flow parameters and dimensionless numbers

Physical meaning	Law	Parameter
Thickness of the penetrated fluid layer near the wall	$\delta_{st} = \sqrt{\frac{2\nu}{\omega}}$	Stokes boundary layer
The ratio of oscillatory inertia to convective inertia	$St = \frac{\omega L}{U}$	Strouhal number
Characterises the balance between unsteady inertia and viscosity	$Wo = \sqrt{\frac{\omega R^2}{\nu}}$	Womersley number
The ratio of the oscillatory inertia force to the viscous forces	$Re_s = \frac{\lvert U \rvert \delta_{st}}{\nu}$	Oscillatory Reynolds number

3.1. Oscillatory flow mechanism

Oscillatory flow is a distinctive type of unsteady flow in which the fluid velocity periodically reverses direction over time. In such flows, heat transfer is governed not only by conventional axial advection and thermal diffusion but also by additional mechanisms induced by oscillatory motion. Compared with constant-flow systems, these processes significantly enhance fluid mixing and thermal transport, often improving heat transfer performance. Unique thermal transport phenomena, including forward advection, reverse advection, and both inward and outward radial diffusion, are caused by the fluid's cyclic back-and-forth motion. As illustrated in Figure 2, the heat transfer mechanism under oscillatory flow can be decomposed into four consecutive stages that recur during each oscillatory cycle. In the forward advection phase (Fig. 2a), thermal energy is convected axially from the hot region toward the cold zone. During the outward radial diffusion phase (Fig. 2b), accumulated heat in the core diffuses toward the cooler tube walls, thereby weakening the thermal gradient. When the flow direction reverses, the reverse advection phase (Fig. 2c) occurs, in which the fluid motion toward the hot zone enhances thermal mixing by transporting residual heat in the opposite direction. Finally, in the inward radial diffusion phase (Fig. 2d), heat diffuses from the reheated walls back into the tube core, re-establishing the temperature gradient and enabling the cycle to restart. This continuous alternation between advection and diffusion processes promotes intensive thermal mixing, leading to a more uniform temperature field within the flow domain. The mechanism offers a crucial explanation for the improved heat transfer performance observed in oscillatory systems and is particularly relevant in applications such as regenerators and thermoacoustic heat exchangers.

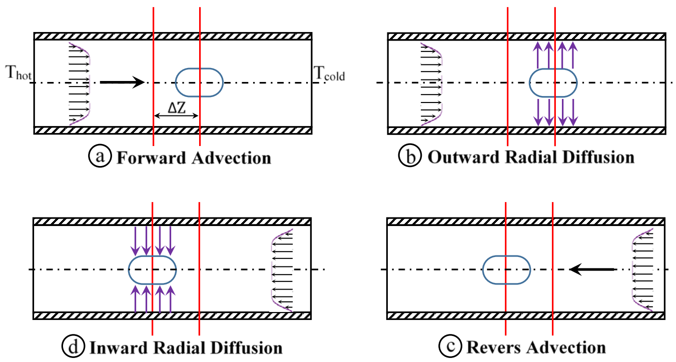

Figure 2. Sequential stages of oscillatory flow thermal transportation

After introducing the basic principles of oscillatory flow and its types, it is essential to discuss significant studies examining its characteristics and mechanisms. Yin et al. [6] proposed an analysis model for oscillating laminar flow inside a capillary tube based on a uniform heat flux boundary condition. Their solution yielded analytical expressions for the velocity and temperature profiles and for the corresponding Nusselt number. The governing parameters for heat transfer were the dimensionless oscillation frequency, oscillation amplitude, and Prandtl number. One key finding was a nonlinear interaction between these parameters. They demonstrated that, under certain conditions, the oscillation significantly increased the Nusselt number, particularly at intermediate frequencies and higher amplitudes. However, their analysis was limited to smooth tubes and steady heat flux conditions, without considering geometrical effects or unsteady boundary heating, which are the focus of the present study.

Xu et al. [7] experimentally analysed the pulsating nanofluid flow in a three-layered microchannel heat sink made by 3D printing. They demonstrated that square-wave pulsing had the best thermal performance, with duty cycles of about 30% producing the most significant improvement (~22%) and increases in the Nusselt number of up to 16.5% compared with steady flow. These results demonstrate the effectiveness of oscillatory forcing in enhancing temperature homogeneity and convective heat transfer in small systems. Nevertheless, the study was confined to microchannel configurations and did not explore the coupling between oscillatory flow and periodic wall geometry. Wantha [8] conducted a comprehensive experimental study on the behaviour of finned tube heat exchangers during unsteady, pulsating airflow. The experimental design varied the pulsation frequency (10–50 Hz), amplitude (13.33%–15.35%), Reynolds number, and blockage ratio to investigate their impact on the average heat transfer coefficient and the Nusselt number. The results demonstrated a significant improvement in the thermal performance of the finned heat exchanger under pulsating flow conditions compared to steady flow conditions. One of their significant contributions was deriving an empirical correlation to estimate the Nusselt number for pulsating flow. The correlation given was found to be correct to ±12.3% when tested against experimental data.

Oscillatory flow has been studied in real-world cooling applications and in investigations of tubes and channels. A recent study by Liu et al. [9] used a combination of CFD and tests to study two-phase oscillating flow in piston cooling galleries. The findings demonstrated a periodic variation in the heat transfer coefficients, which reached a maximum of 2536 W/m²·K at the bottom wall. While lowering the injection pressure by 100 kPa reduced the heat-transfer coefficient(HTC) by more than 11%, increasing the nozzle diameter from 1.8 to 2.0 mm increased the average HTC by 4–12%. These results indicate that, when it comes to regulating oscillatory heat transfer performance, geometric factors such as nozzle size are more significant than injection pressure.

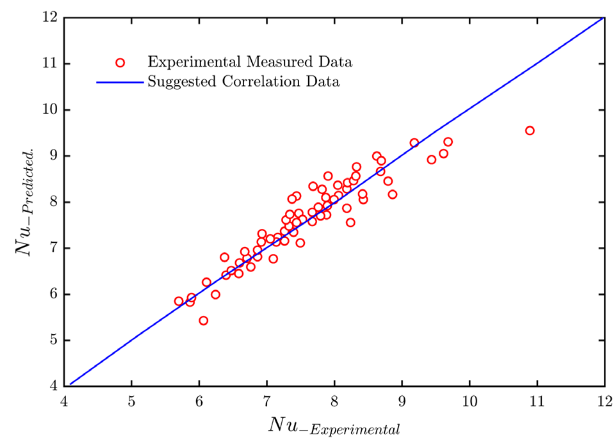

Figure 3. Measured and predicted Nusselt number

Pendyala et al.[10] conducted an experimental investigation to find the influence of low-frequency axial oscillations on single-phase flow convective heat transfer in a vertical tube. The experimental setup involved placing the tube on a mechanically oscillating table and subjecting a middle section of the tube to a constant heat flux. The study revealed that oscillatory motion significantly enhanced the heat transfer coefficient during the laminar regime; however, no significant effect was observed during the turbulent regime (Re > 2100). Enhanced flow perturbations and increased mixing were caused by oscillations. The study established a correlation between the local Nusselt number and the Reynolds number. The employed empirical correlations for laminar oscillatory water flow ($500 \le Re \le 2100$, $Pr \approx 6$) under constant heat flux. The correlations are valid for single-phase flow and do not account for axial conduction effects. The deviation between the predicted and experimental data is within ±11.4 %, as shown in Figure 3 as a parity plot [10].

Patil and Gawali [11] conducted a thorough experimental study of heat transfer characteristics in an oscillating fluid flow within a circular tube to evaluate the effect of various flow and thermal parameters. Unlike the majority of studies that focus solely on sinusoidal boundary conditions, the present study tested multiple combinations of oscillation frequencies, tidal displacement amplitudes, and heat flux levels. The primary outcome was the derivation of an experimental correlation for the effective thermal conductivity in terms of the parameter S^2,. The correlation facilitates predicting the optimum heat-transfer condition before the transition to turbulence. They demonstrated that the enhancement of heat transfer was most effective within specific ranges of displacement and frequency, thereby confirming the existence of a critical oscillatory regime. Additionally, the excitation produced by highly fluctuating velocity gradients in rapidly developing flows was found to be the dominant mechanism for enhancing axial transport. Oscillatory flow more effectively reduces axial temperature gradients and produces more uniform temperatures than steady flow.

Jalil [12] developed a mathematical model by conducting 2D axisymmetric numerical simulations to study the conditions of perfect or near-perfect thermal mixing between two reservoirs, A and B, connected by a duct under oscillatory flow. The results were derived analytically from fluid displacement dynamics and validated through computational simulations for 24 test cases. Based on the oscillation parameters and fluid displacement behaviour, five regimes of mixing quality were identified, and it was determined that optimal perfect mixing is achieved at a normalized axial displacement () when the thermal mixing ratio was 97% to 100% ($\zeta_2 / \zeta_1 = 1$), as shown in Figure 4b [12], where the flow inside the reservoirs will be perfectly mixed and circulated. A new correlation was proposed to predict heat transfer augmentation under oscillatory exchange as a function of Reynolds number, displacement amplitude, and frequency.

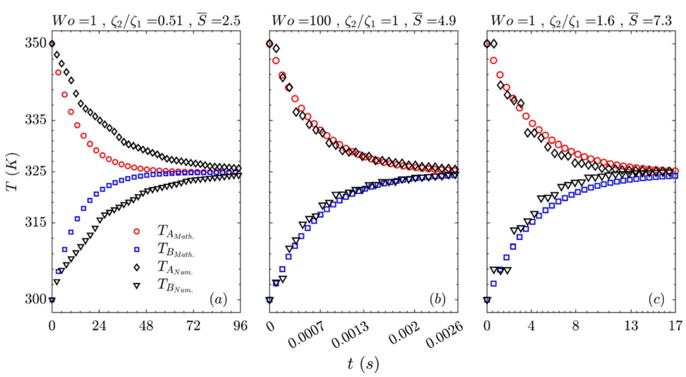

Figure 4. Oscillatory flow mixing quality types: **(a)** poor, **(b)** perfect, and **(c)** extra mixing

Liu et al. [13] performed a numerical investigation of the thermal and fluid dynamic responses of two tandem cylinders subject to an oscillating inlet velocity. The most significant finding is that oscillatory flow significantly improves heat transfer for both upstream and downstream cylinders. The heat transfer enhancement is highly sensitive to the synchronization between the oscillation frequency and the vortex-shedding cycle, a phenomenon known as the resonance effect. Kamsanam et al.[14] conducted an in-depth experimental investigation to evaluate the thermal performance of finned-tube heat exchangers under oscillatory flow, directly applicable to thermoacoustic systems. The experiments measured heat transfer effectiveness and the Nusselt number for various acoustic displacement amplitudes and frequencies. The main contribution of the work is the determination that a fin spacing of about 2–4 times the thermal penetration depth yields optimal performance. It shows that longer fins are not always the best choice, as they create flow blockage and reduce local mixing. They also provided a validated empirical correlation for application in realistic engineering design under oscillatory thermal conditions.

Jalil [15] the effect of dissipative bulk heating can be described by a proposed correlation in terms of Womersley number (Wothe effect of dissipative bulk heating can be described by a proposed correlation in terms of Womersley number (Wo conducted a numerical study focusing on a relatively underexplored yet critical phenomenon in oscillatory flow: viscous heat dissipation (Φ). The study examined how internal friction in the fluid, particularly in oscillatory airflow and thereby potentially affects the performance of heat exchangers. The study analysed laminar, oscillatory airflow between two reservoirs connected by a smooth tube of length L, considering various Womersley numbers and axial tidal displacements (ΔZ). The main contribution of the work is the introduction of a new threshold criterion that clearly defines when viscous heat dissipation(VHD) becomes significant enough to affect the thermal field, as illustrated in Figure 5 [15]. This concept had not been systematically established in previous research. The study found that below a particular combination of Wo and ΔZ, the effect of VHD can be safely neglected. As Wo and ΔZ increase, the bulk fluid temperature rises, and a correlation , based on flow parameters, is proposed to quantify the contribution of VHD to the temperature field.

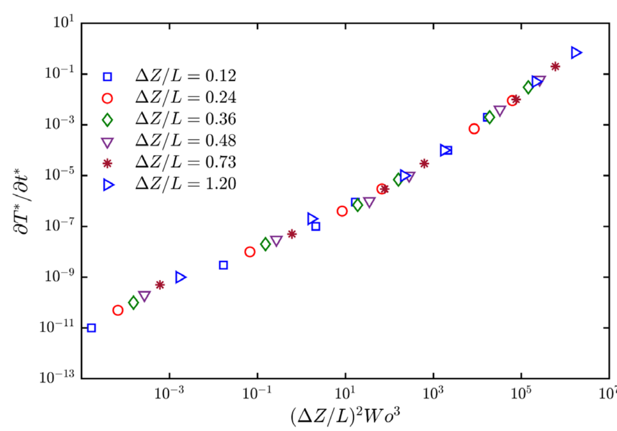

Figure 5. Variation of normalized unsteady temperature rate at different axial tidal displacements

A combined experimental and numerical investigation by Jalil[16] provided one of the most comprehensive assessments of axial heat transfer under laminar oscillatory flow between thermal reservoirs connected by a multi-tube bundle. Experimentally, a multi-tube test rig was constructed, and sinusoidal oscillations imposed using a controlled piston. The results from both approaches were compared and found to be in good agreement, reinforcing the validity of the numerical framework. Two significant empirical correlations are proposed: for high Womersley numbers (Wo > 3), the effective axial thermal conductivity scales as $k_{eff} \propto Wo^{1.62,}$ and for low Womersley numbers, the enhancement behaves exponentially and depends strongly on tidal displacement (ΔZ) and the pressure-gradient amplitude. Brereton and Jalil [17] investigated the enhancement of axial heat and mass diffusion resulting from laminar oscillatory pipe flow in the presence of axial temperature or concentration gradients. Oscillatory flow introduces cyclic convective motion that couples with radial diffusion to produce time-averaged axial transport rates that are orders of magnitude higher than those achieved through molecular conduction or diffusion alone. The analysis assumes zero net mass flow, focusing on fully developed laminar oscillatory flow in a pipe. The key result is that the enhanced diffusivity scales quadratically with the amplitude of the pressure gradient and the Prandtl (or Schmidt) number, and exhibits a bimodal dependence on frequency:

- At low frequencies(Wo < 1),the system exhibits quasi-steady behaviour, and enhanced diffusivity increases rapidly with Wo.
- At high frequencies (Wo > 10), diffusivity decays following a power-law trend due to the diminished penetration depth of the oscillatory motion into the fluid (linked to the Stokes layer thickness).

According to Figure 6 [17], the optimal heat transfer improvement for most fluids occurs at a Womersley number of approximately three.

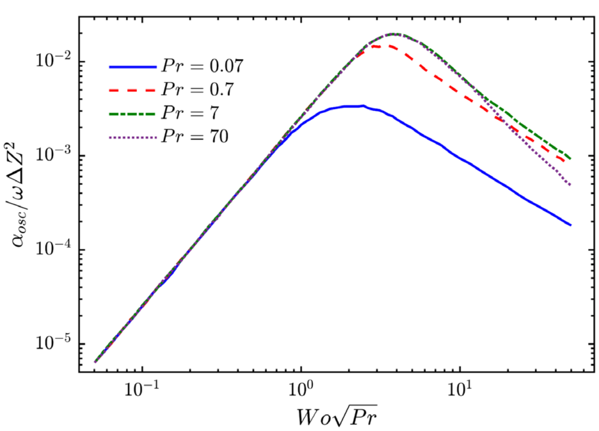

Figure 6. Variation of axial thermal diffusivity at different Prandtl numbers

Brereton et al. investigated the response of an oscillatory-flow heat exchanger explicitly designed to optimize axial heat transfer with no net mass flow. The research verifies these theoretical estimates experimentally in water and other liquids across a range of oscillation frequencies. The experimental results showed that the oscillatory thermal conductivity was enhanced to approximately 30,000 times the fluid's molecular conductivity, resulting in efficient axial thermal conductivity. The unit heat flux corresponding to a unit temperature gradient was approximately 70,000 W/m²·K, comparable to advanced cooling methods, such as submerged liquid jet impingement, and significantly higher than that of conventional air-cooled heat sinks or constant liquid-convection systems. Additionally, the authors attribute the enhanced heat transfer to two primary parameters: oscillation frequency, which directly impacts the Womersley number, and tidal displacement, which governs the size of the fluid mass oscillated in each cycle. They also highlight a physical mechanism for enhancing heat transfer.

Brereton and Jalil investigated the behaviour of axial heat conduction in oscillatory laminar flow within pipes analytically, with a particular emphasis on the limits of axial linear temperature assumptions. The authors begin by solving the governing equations for fully developed, oscillatory laminar flow under a sinusoidal pressure gradient. When dissipation is neglected and axial temperature variation is assumed linear at any instant, exact solutions are obtained for the unsteady velocity and temperature fields, axial heat flux, and effective thermal conductivity. However, the authors demonstrate that these solutions become invalid at low Womersley numbers (Wo < 0.1) because the instantaneous axial temperature variation is no longer linear, which breaks a key assumption of the analytical model. To address that, a quasi-steady thermal model is proposed. The quasi-steady model becomes increasingly accurate as Wo approaches zero. At high Womersley numbers (Wo > 5), the study shows that dissipation effects (viscous heating) become significant. The authors derive a simple criterion, based on fluid properties, oscillation frequency, and geometric parameters, to predict when dissipation must be accounted for. One of the most significant contributions of the work is the identification of two distinct breakdown regimes for analytical solutions: one caused by nonlinearity in axial temperature at low Wo, and the other by viscous dissipation at high Wo.

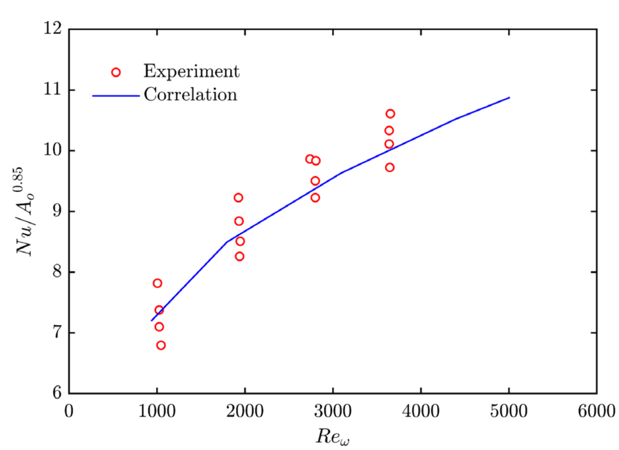

Figure 7. Correlated and measured cycle-averaged Nusselt number at different oscillatory Reynolds numbers

Akdag and Ozguc [20] quantified the heat-transfer performance of a vertical annular flow channel subjected to pure oscillatory flow (zero mean mass flux) to determine how oscillation parameters influence convective heat transfer. The experiments independently tested three key parameters: oscillation frequency (four values), oscillation amplitude (three values), and imposed heat flux (three levels). From the experimental data, the authors calculate cycle-averaged Nusselt numbers using a control-volume energy balance and time-averaged temperature profiles. A key contribution of the study is the derivation of an empirical correlation that expresses the cycle-averaged Nusselt number as a function of the oscillatory Reynolds number (ranging from 1000 to 4000) and the oscillation amplitude (7.73-12.88), as shown in Figure 7 [20]. The heat transfer performance (represented by the Nusselt number) increases with both oscillation frequency and amplitude. This enhancement is attributed to intensified unsteady convection and near-wall mixing induced by higher oscillatory velocities. Consequently, under specific combinations of Re_{ω} and A_{o}, the cycle-averaged Nusselt number surpasses that of equivalent steady-flow cases, particularly in systems with small hydraulic diameters and short flow passages, where boundary-layer interaction effects are most pronounced.

Akdag et al. [21] investigated the heat transfer performance of oscillating liquid columns within vertical annular channels experimentally. To determine the general features of convective heat transfer, the analysis utilizes cycle-averaged temperatures and heat fluxes. As illustrated in Figure 8 [21], the results are stated in terms of the Nusselt number(Nu),which has an empirical correlation with the kinetic Reynolds number (Re_{ω}). The Nusselt number clearly increases with Reω in the figure, suggesting that higher oscillatory velocities promote stronger convective mixing and thinner thermal boundary layers. This result demonstrates that in contrast to stable or static conditions, oscillatory motion improves heat transfer efficiency. In settings with constrained geometries such as narrow annular tubes where wall interactions enhance fluid velocity and heat transfer, this amplification is most noticeable. Patil and Gawali [22] experimentally evaluated the heat transfer performance of an oscillatory flow heat exchanger using a piston-cylinder setup with water as a working fluid. The heat transfer was characterized by measuring axial heat flux, effective thermal conductivity (k_{eff}), and convective heat transfer coefficient (h) under various oscillation regimes. A key observation was that k_{eff} increases with frequency up to an optimal point and then decreases. Additionally, increasing tidal displacement shifts this optimal point to lower frequencies. Based on these findings, the authors introduce a new empirical correlation for the effective thermal diffusivity α_{eff} as a function of Womersley number and a derived transition number (β). This correlation allows for the accurate prediction of thermal enhancement under practical conditions.

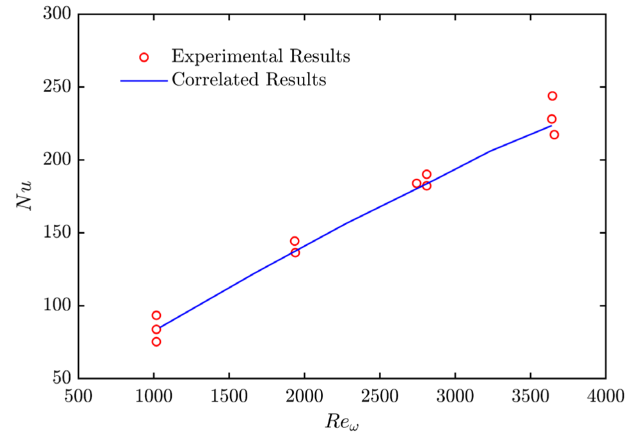

Figure 8. Nusselt number improvement with kinetic Reynolds number

Tang et al. [23] studied the oscillating flow heat transfer in a finned heat exchanger used in pulse tube refrigerators. They conducted a detailed experimental investigation of space-cycle-averaged Nusselt numbers under varying Reynolds and Valensi numbers. The flow is strictly laminar and oscillatory, with zero mean mass flow. Two characterizations are used to describe heat transfer: complex Nusselt numbers capture phase differences between oscillating wall heat flux and temperature, while space-cycle-averaged Nusselt numbers provide a time-averaged measure of practical performance. The authors propose a new empirical correlation that relates the Nusselt number to the maximum Reynolds number and the Valensi number, showing agreement(within 6.3%)with experimental results. Luo et al. [24] presented a 2D numerical simulation of laminar flow over an oscillating cylinder, analysing how oscillation parameters (amplitude, frequency, and angle) influence convective heat transfer. Simulations are run at Re = 197–296, covering typical pre-transitional regimes, and use the field synergy principle to interpret the results. Key findings show that an increase in amplitude has a strong positive effect on heat transfer due to intensified vortex shedding; frequency effects are more complex, with the Nusselt number initially decreasing and then increasing as frequency increases; and optimal oscillation angles are around 0° and 90°, where synergy between velocity and temperature gradients is maximized.

3.2. Phase lag in oscillatory flow

An essential feature of unsteady pulsating or reciprocating flows is the phase lag between their parameters. It is the angular delay between important flow parameters, such as velocity, the pressure gradient, and the wall shear stress. The interplay of fluid inertia, viscous effects, and turbulent structures in oscillatory turbulent pipe flows gives rise to complex phase relationships that vary significantly across the pipe radius. Numerous experimental and numerical investigations have examined the radial variation of phase lag in unsteady flows, especially under various frequency regimes and flow conditions. Jalil [25] conducted a numerical study on the phase interactions (Φ) between centerline velocity (u_{cL}), wall shear stress

(τ_w), and pressure gradient in a pulsating turbulent flow through a smooth circular tube. The study examined the part of the tube cross-section where the radial phase lag varied. For $\omega^+ > 0.06$, the phase lag between velocity and pressure gradient increased from the wall towards the centerline compared with that observed at lower frequencies. At the same time, it reduces the shear-stress lag by up to 280° at specific points along the centerline. The velocity lags the pressure gradient by 45° at the centerline and by up to 90° near the wall. Shemer et al.[26] presented an experimental investigation comparing turbulent and laminar pulsating flows in a straight smooth pipe of 33 mm diameter and 16.5 m length (500D). Measurements were primarily conducted at a mean Reynolds number Re = 4000 (range 2900 < Re < 7500) and pulsation periods from 0.5 to 5 seconds. In both laminar and turbulent regimes, pulsations caused only slight changes in time-averaged parameters, including velocity profiles and friction factors. A sophisticated eddy-viscosity model was presented to account for the observed phase delays. The authors found that turbulence exhibits memory effects and non-trivial responses, which depend on frequency and Reynolds number (Re). The amplitude and phase distributions in turbulent pulsating flow significantly deviate from those in laminar flow, while the mean flow remains unaffected.

Mankbadi and Liu [27] studied a turbulence model based on rapid-distortion theory to predict the near-wall unsteady response in turbulent shear flows exposed to oscillating pressure gradients. The study focuses on high-frequency forcing where quasi-steady models fail. Key findings include that the modulated wall shear stress exhibits a phase lead of ~45° and deviates from the Stokes solution. The amplitude peaks of turbulent kinetic energy shift closer to the wall and decay with increasing frequency. The results confirm that the phase and amplitude of turbulent quantities diverge from those of the oscillating mean flow with increasing ω^+, making quasi-steady or eddy-viscosity models inadequate near the wall. Rosenberg et al.[28] investigated the phase behaviour of turbulent boundary layer quantities excited by a 50 Hz wall-actuated roughness element at free-stream velocity U_∞ = 22.4 m/s, boundary layer thickness $\delta \approx$ 17 mm, Reynolds number Re ≈ 3100, and friction Reynolds number $Re_\tau \approx 990$. Experimental phase lags of up to 20° between velocity and shear, and about 140° between pressure and shear, were observed during phase calibration in a plane wave tube operating at frequencies between 300 and 1900 Hz. According to theory, in boundary-layer investigations, wall pressure leads the shear by about 140°, while velocity leads the shear by about 20°. Brereton and Mankbadi[29] presented a rapid-distortion-theory turbulence model for fully developed unsteady wall-bounded flow, particularly tested on turbulent pipe flow with sinusoidal streamwise oscillations. Experiments used a 57-mm-diameter, 160D-long pipe at Re = 11,700, with oscillation frequencies ranging from 0.25 to 4 Hz and centerline oscillation amplitudes varying from 19% to 11% of the mean velocity. The results showed that the wall shear stress phase lag approached the 45° Stokes solution at high ω^+, and it reasonably matched the oscillatory velocity and turbulent stresses in the near-wall region.

Mishra and Girimaji [30] presented the problem of simulating the pressure-strain correlation, which is fundamentally non-local, in a single-point turbulence closure framework. The model accurately predicts Reynolds stress anisotropy and turbulent kinetic energy, particularly in elliptic flows, where conventional models fail, while maintaining realizability across large regions of anisotropy space. Overall, the study represents a significant advancement toward robust, single-point turbulence modelling with enhanced physical fidelity. Figure 9 shows the relationship of phase difference between the shear stress and the centerline velocity) $\phi_{\tau w} - \phi_{uCL}$(as a function of the dimensionless frequency ω^+. The figure compares previous experimental and numerical studies. The results show that as the frequency increases, the phase lag rises and eventually stabilizes at around 45° for $\omega+ > 0.06$. This behaviour indicates that at high pulsation frequencies, the centerline velocity increasingly lags behind the wall shear stress. A discernible disparity is observed among several experiments at low frequencies, indicating the complexity of the flow response. The dynamic behaviour of oscillatory flows is consistent with the phase lag tending to stabilise as frequency increases. These discrepancies highlight the importance of methodical research to better understand the underlying mechanisms.

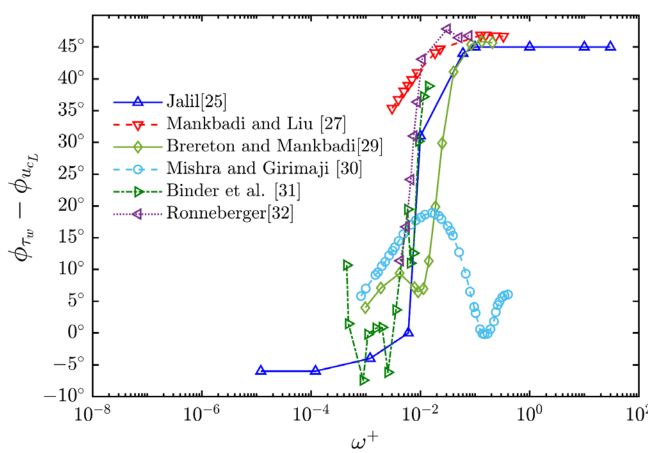

Figure 9. Phase lag between the wall shear stress and the centerline velocity

In addition to the studies reviewed and summarized above, Table 2 provides a comparative overview of previous experimental and numerical investigations that specify the phase lags among the pressure gradient, velocity, and wall shear stress under oscillatory flow conditions. The ranges of important dimensionless parameters (for example, dimensionless frequency and the Womersley number) and their associated phase differences, as documented in the literature, are highlighted in the table below. It serves as a guide for understanding the common phase lag behaviour observed in various flow regimes and modelling techniques. There are notable differences at low and middle frequencies, although there is often agreement at higher frequencies. These discrepancies indicate that further investigation and experimental validation are necessary to establish more robust correlations. Table 3 presents a comprehensive comparison of previous studies investigating oscillatory flow characteristics under different operating conditions and geometrical configurations. The table lists all essential parameters and presents the primary finding within a specific range. The findings from various studies indicate that experimental settings inadequately cover a wide range of oscillation frequencies and axial displacements.

Table 2. Oscillatory flow parameters phase lag at different fluctuating rates

Ref.	Range	Phase lag (Φ)
[25]	$1.2\times10^{-5} \le \omega^{+} \le 33.5$	$\Phi_p - \Phi_u = 0°$ to $90°$ $\Phi_p - \Phi_{\tau w} = 0°$ to $\sim 90°$ $\Phi_{\tau w} - \Phi_{ucL} = 0°$ to $45°$
[26]	$4.5 \le Wo \le 15$	$\Phi_p - \Phi_u = 30° - 85°$
[27]	$0.0015 \le \omega^{+} \le 0.12$	$\Phi_{\tau w} - \Phi_{uc} = 45°$
[28]	$300 < f < 900$	$\Phi_{\tau w} - \Phi_u = 45° - 61°$
[31]	$0.0004 \le \omega^{+} \le 0.16$	$\Phi_{\tau w} - \Phi_{uc} = (-4°) - 36°$
[32]	$0.004 \le \omega^{+} \le 0.097$	$\Phi_{\tau w} - \Phi_{uc} = 11° - 47°$
[30]	$0.2 \le St \le 5$	$\Phi_{\tau w} - \Phi_{uc} \approx 6° - 20°$
[29]	$0.01 \le \omega^{+} \le 0.16$	$\Phi_{\tau w} - \Phi_{uc} = 4° - 45°$
[33]	$0.004 \le \omega^{+} \le 0.046$	$\Phi_u - \Phi_{imposedflow =} (-15°) - 12°$ $\Phi_{\bar{u}} - \Phi_{imposedflow} = 0° - 375°$ $\Phi_{\bar{v}} - \Phi_{imposedflow} = 50° - 385°$
[34]	$0.001 \le \omega^{+} \le 0.01$	$\Phi_{\bar{u}\bar{v}} - \Phi_{uc} = (-250°) - 50°$ $\Phi_p - \Phi_\tau = 50° - 135°$
[35]	$0.043 \le \omega^{+} \le 0.34$	$\Phi_u - \Phi_{uc} = 0° - 45°$ $\Phi_{\bar{u}} - \Phi_{uc} = (-1°) - (-8°)$

Table 3. Previous Oscillatory flow investigations categories, parameters, limitations, and findings

Ref.	Approach	Surface Type (Smooth/ Periodic/etc).	length	Flow Parameters (Wo, f, ω, St, Re)	Key findings
[6]	**Analytical**	Circular pipe (capillary round tube).	- Normalized	- ω^*=0.1 - 1.0. - A= 0.0001 - 1.0.	-The peak Nusselt number depends on frequency (ω^*) and amplitude (A): When A=0.1 and ω^*=1, Nu increases from 8.318 to 52.22. -When ω^* increases, the oscillation effect on heat transfer diminishes. -At high oscillation frequencies, the enhancement effect disappears. -For small amplitude (A<0.01), heat transfer is similar to steady flow, and for larger amplitude (A>0.1), oscillatory flow enhances heat transfer.
[8]	**Experimental**	-Finned tube heat exchanger with straight fins. -Two configurations were tested: -HX-01: 11 fins, blockage ratio (Br) 95.2% -HX-02: 21 fins, blockage ratio 91%	- 140 mm	- f= 10–50 Hz - 192 ≤ Re ≤ 2069	-The average Nusselt number (Nu) in pulsating flow was significantly higher than in steady flow. -Nusselt number enhancement up to 136% at f = 15 Hz. -The maximum enhancement occurred at 15–20 Hz. -Higher amplitude increased instability and heat transfer. -With Re = 253, f = 30 Hz: -Nu increased by 21.6% (A = 13.35%). -Nu increased by 25.5% (A = 14.48%). -Nu increased by 31.7% (A = 15.23%).
[25]	**Numerical**	Smooth circular tube.	- 0.5 m	-Wo= 0.7 - 2069. - $\omega^{+}= 1.2 \times 10^{-5}$ to 33.5. - St: 5.3×10^{-5} to 531 - Re = 5115 - Re_δ= 2 to 6083.	- At high frequencies ($\omega^{+} > 0.06$), the phase lag increases radially from the wall to the tube center. -Centerline velocity lags the pressure gradient by 90°. -Wall shear stress lags the pressure gradient by 45°. - Shear stress lags behind the pressure gradient by up to 280° in the core. -A thin oscillatory boundary layer (Stokes layer) forms at high frequencies. -Reverse flow occurs when the oscillatory amplitude (A) exceeds 0.3
[10]	**Experimental**	Smooth vertical tube.	- 1.75 m - 0.55 m heated section.	- f= 0.125–0.5 Hz. - 500 ≤ Re ≤ 6,500	-Nusselt number increased by up to 60.3% at Re = 567, acceleration = 1.125 m/s². -Higher oscillation acceleration enhances heat transfer.

[11]	**Experimental**	Small circular tube.	- 1.34 m cooling tube. - 0.15 m heated section.	- f= 0.25 to 2 Hz. - $1005 \leq \beta \leq 4177$ - $4.7 \leq$ Wo ≤ 16.24	- The convective heat transfer coefficient (h) increased with decreasing frequency. -Maximum h observed at f = 0.25 Hz due to longer interaction time between the stagnant boundary layer and the moving liquid core. - Larger S leads to higher heat transfer enhancement. -For S > 2.67 m, the thermal boundary layer became unstable, leading to early turbulence.
[12]	**Analytical and Numerical**	A short duct connects two reservoirs.	- The study focuses on normalized axial displacement (S).	- $1 \leq$ Wo ≤ 100 - Re ≤ 850	-Perfect mixing achieved at S = 4.9 with mixing ratio 97%–100% -Effective thermal conductivity (k_{eff}) increased up to $O(10^6)$ times compared to molecular conductivity. -Heat transfer improved by 160% compared to the perfect mixing case under specific conditions.
[13]	**Numerical**	Two circular cylinders are arranged in tandem.	- Single-cylinder case: 30D (length) × 20D (width). - Two-cylinder case: 35D (length) × 20D (width). - Distance between cylinders: 5D.	- Cycle ratio: 0.50 to 1.05 - Amplitude ratio: 0.25 - 1.00. - Re=200	-Upstream cylinder: Maximum heat transfer enhancement at $T_{inlet}/T_{vortex} = 0.90$. - Downstream cylinder: Peak enhancement at $T_{inlet}/T_{vortex} = 0.90$ and 0.50. - Oscillating inlet flow improved heat transfer without increasing the coolant flow rate. - Heat transfer enhancement reached up to 20%.
[14]	**Experimental**	Finned-tube heat exchanger.	- Fin length: 20 mm. - Total resonator length: 8.9 m.	- Ao: 0.04 to 2.15.	- Nusselt number (Nu) increased with displacement amplitude. -Peak heat transfer observed at normalized gas displacement amplitude $(\xi_a - g)/(\sigma L) \approx 0.5$.
[15]	**Numerical**	Tube with reservoirs	- 100 mm	- $0.1 \leq$ Wo ≤ 100 - $Re_s < 850$	-The VHD (Viscous Heat Dissipation) effect is negligible if $(DZ/L)^2 Wo^3 < 10^3$ -At high frequencies, the VHD effect becomes more pronounced due to the thinner Stokes boundary layer
[16]	**Experimental and Numerical**	Circular tubes connect hot and cold reservoirs.	- 100 mm	- $0.1 \leq$ Wo ≤ 100 - $Re_s < 850$	- Axial heat transfer enhancement: More than 10 times with conductive tube walls. -Oscillatory thermal conductivity (k_{osc}): Enhanced by five orders of magnitude compared to molecular thermal conductivity -Wall thickness improves heat storage release, increasing heat transfer up to 10 times for small thicknesses. -Axial conduction effect: Becomes negligible for Wo > 3
[17]	**Analytical**	Circular pipe.		- $0.1 \leq$ Wo ≤ 100 - $Re_s > 500$ for Wo > 10	- Enhancement follows a quadratic dependence on pressure gradient amplitude - Conductive walls can enhance heat transfer by a factor of up to 10 in quasi-steady conditions. -The optimal frequency for maximum enhancement occurs at Wo≈1
[36]	**Experimental and Analytical**	Oscillatory-flow heat exchanger with tube matrix.	- 250 mm	- $0.5 \leq$ Wo ≤ 10	-Axial thermal conductivity enhancement (k_{osc}/k): Up to 30,000 times greater than molecular conductivity -peak thermal conductance (h): 70,000 W/m²·K at Wo≈8 - Steady-state heat flux: 1 kW achieved at 5 Hz oscillation frequency. - Effect of nanoparticle additives: Increased molecular conductivity by 20%, but no significant impact on oscillatory enhancement
[19]	**Analytical and Numerical**	Circular pipe.	- 20D	- $0.005 \leq$ Wo ≤ 50	- The unsteady temperature field is invalid at low Womersley numbers because the momentary axial variation of temperature is not linear - When dissipation is significant, exact solutions for the unsteady temperature field are invalid at high Womersley numbers because the momentary axial variation of temperature is also nonlinear.
[20]	**Experimental**	Annular channel.	- 2m	- ω= 1.445 to 5.130 rad/s - A_o: 7.73 to 12.88 - Re_ω=1000 to 4000	-Heat transfer increases with both frequency and amplitude of oscillation -Nusselt number enhancement: Increased up to 90.22 at Re_ω=3642.88 and A_o=12.88
[21]	**Experimental**	Vertical annular channel	- 2m	- ω= 1.435 - 5.131 - Re=1,019 - 3,643	- Nusselt Number (Nu): 74.89 - 242.10 - Heat Removal Rate: Increases with oscillation frequency

[22]	**Experimental**	Oscillating flow heat exchanger (tube)	- 0.5 m (flow tube) + 1.34 m (cooling tube in heat sink)	- 11.44 ≤ Wo ≤ 27.87 -Tidal Displacement (S): 0.417 - 1.833 m	- Effective Thermal Conductivity (k_{eff}) increases with frequency up to an optimum and then decreases. - Axial Heat Flux (also increases with frequency before reaching a peak.
[23]	**Experimental**	Finned heat exchanger	- Fin length 20mm	- f= 40 - 110 Hz -Valensi Number (Va): 150 - 350 - Velocity Amplitude: 0.5 - 3.8 m/s - Re=200-1200	-Nusselt Number (Nu): 5.0 - 8.3 -Nu increases with increasing Re_{max} and Va
[24]	**Numerical**	Circular cylinder	- 200mm	-f (Hz): 1 - 5 - A: 2 - 10 mm -Oscillating Angle (ϕ): 0° - 90° - Re=197, 248, 296	- (Nu): Increased by 53.43% for A=10mm and Re=197 - Increasing f from 1 Hz to 5 Hz improved Nu by 42.13% at Re=197 - The best enhancement at ϕ=90∘ yields a 66.74% improvement - Single vorticity lines became disordered at higher amplitudes
[37]	**Experimental and Analytical**	Rectangular channel.	- 300 mm - Width = 30 mm - Height = 4.2 mm.	- f= 0.02, 0.1, 1, and 10 Hz - 1.49 ≤ Wo ≤ 33.33 - Re_s=34	-Pulsating flow enhanced heat transfer by up to 40% -Pressure drop increased due to inertial losses, leading to high operational costs at high frequencies -Increased wall shear stress at high frequencies, indicating improved convective cooling -Higher pulsation frequencies caused plug-like flow, thinning the Stokes layer to 1 mm at Wo=33.3
[38]	**Analytical**	Circular pipe (tube).	NA	- f= 1.4 Hz – 17 Hz. - ω= Given as 2π/3in the base case (0.17 Hz). - Re=780-1987	-Pulsating laminar flow can reduce the average heat transfer. -The reduction is more significant at low frequency, high pulsation amplitude, large wall heat capacity, and small Prandtl number. - The fluctuation of temperature and heat flux decreases with a high Prandtl number. -The pulsation effects are more prominent for pipe flow than for flow between parallel plates.
[39]	**Analytical**	Circular pipe (capillary round tube).	- Normalized	- ω^* = 0.1-10	-The triangular pressure waveform enhances heat transfer more than the sinusoidal waveform. -For a triangular pressure waveform, the peak Nusselt number can reach 18.08, compared to 5.140 for a sinusoidal waveform at the same frequency and amplitude. -When the frequency increases, the peak Nusselt number decreases (from 18.08 to ~4.4 when ω^*=10). -When the amplitude increases, the peak Nusselt number increases significantly (from 4.386 to 17.53). -At high oscillation frequencies, the pressure waveform's effect on heat transfer disappears.
[40]	**Analytical**	Circular pipe and two-dimensional channel.	- Normalized	- Slow oscillations (ω→0) - Fast oscillations (ω→∞)	-The rate of mass transfer is significantly enhanced in oscillatory pipe flow compared to steady flow. -Higher frequency leads to greater mass transfer enhancement. -For high-frequency oscillations: -The enhancement is proportional to sqrt ω.
[41]	**Experimental**	Finned-tube heat exchanger with various fin spacings: 0.7 mm, 1.4 mm, and 2.1 mm.	- 8.9 m - Fin length 20mm	-Gas displacement amplitude ranges from 0.03 to 1.5 - 10 <Re_o< 10000	-Optimal normalized fin spacing (D/dk) found between 5.0–5.5 -Optimal normalized gas displacement amplitude: 0.5
[42]	**Experimental**	Circular tube	- 1.2 m	-Wo=1-10 - Re/α up to 300,	-Axial dispersion rate reduced as oscillation frequency increased -The transition to turbulence was not observed within the tested range despite reaching Re/α of 300
[43]	**Numerical**	Pulse tube refrigerator (PTR) with heat exchangers (HEs).	- Cold end=20mm - Hot end=10mm - Pulse tube=60mm	- f = 40 Hz (base case). - Phase angle (θ) varied from 0° to 75° - m_{in} =8.16 kg/m^2 s	-Poor heat transfer in HEs leads to >10% power loss if h decreases to 102 W/m²·K -A 1.2W loss was observed when the heat transfer coefficient decreased significantly -A 0.5mm layer near the tube wall showed high velocity, affecting system performance. -The coldest temperature was 78.57 K at 21 mm, and the highest was 304.92 K at 77 mm.

[44]	**Numerical**	Two heated parallel channels with constant wall heat flux.	- Heated length 3000 mm	- Δt=0.01-0.02 s - Re= 25432 to 37524	- At total flow rate = 0.0340 kg/s, oscillations grow → unstable. -At total flow rate = 0.0342 kg/s, oscillations decay → stable. -Stability threshold mass flow rate values ranged between 0.0327 kg/s and 0.0365 kg/s. - Changing the outlet plenum volume had a negligible effect (<1%) on flow instability boundaries. -The turbulent Prandtl number affected the instability threshold, with values ranging from 0.85 to 1.05
[45]	**Numerical**	Lid-driven square cavity with an oscillating thin fin	- The fin length varies sinusoidally with: -Mean length = 10% of cavity side - Amplitude = 5% of cavity side	- 0.005 $\leq$ St $\leq$ 0.5 - Re=100 and 1000	- The amplitude of fluctuations of the mean Nusselt number on all four walls increases as the fin oscillates slower. - At Re = 1000, TR = 10, a counterclockwise (CCW) vortex forms and moves across the cavity, affecting the temperature field. - The maximum temperature fluctuations (h_{amp}) increase as the fin oscillates slower. -The maximum Nusselt number amplitude increases with Re = 1000.
[44]	**Analytical**	-Horizontal channel with two immiscible viscous fluids -Permeable walls allow transpiration flow	- Infinite parallel plates are assumed	- ω=0.0001 to 10 - Re $\approx$ 0 to 3.4	-Velocity decreases as the viscosity ratio (α) increases. -Velocity increases with higher oscillation amplitude (ϵA) -Temperature decreases with a higher Prandtl number (Pr). -Temperature increases as the frequency parameter ω increases.
[46]	**Numerical**	Bluff Bodies (Circular and Square Cylinders)	- Assumed to be of infinite length.	- Δt=0.001 s - Steady Flow: 20 $\leq$ Re $\leq$ 100 - Unsteady Flow: Re_s = 150-300	- Nu increases with Reynolds number and nanoparticle concentration. - Nu increase rate slows down at higher Re and volume fractions. -Steady Flow: Enhancement ratio: 1.10 – 1.35 -Unsteady Flow (Re = 150, 300): Enhancement ratio: 1.10 – 1.8 -Higher enhancement for square cylinders than circular cylinders in unsteady flow. - Entropy generation decreases with increasing Re.
[47]	**Numerical and Analytical**	Vertical flat plate	- Assumed a thin vertical flat plate	- 1$\leq$ f $\leq$ 10 - Re_s up to 6000	-Enhancement factor E < 2 due to oscillatory motion. -Heat transfer enhancement increases with the frequency and amplitude of oscillation. -The enhancement factor E is highest at the lower Grashof number (Gr). -Oscillatory motion enhances heat transfer by increasing the temperature gradient across the Stokes layer.
[48]	**Experimental**	-SUS 302 Stainless Steel -Tube Inner Diameter: 10 mm -Tube Wall Thickness: 2 mm	- 1800 mm	-Oscillation Period (τ): 1.04 – 11 s -Normalized Amplitude of Oscillation) $\Delta G_{max}/G_{av}$(: 0 – 3.0	- Wall temperature fluctuations increase with the oscillation period and heat flux. - The larger the $\Delta G_{max}/G_{av}$, the lower the periodic CHF. - The effect of pressure (0.5–3.0 MPa) on CHF reduction is minimal. - Higher mass flux (Gav = 170 kg/m²s vs. 100 kg/m²s) results in a greater reduction in CHF due to stronger liquid film thinning.
[49]	**Experimental**	Vertical tube, inner diameter 6.0 mm, heating length 720 mm.	- 1620 mm	- Flow oscillation period (τ): 1.04 – 10.6 s - Mass velocity ratio: 0 – 3.0 - Heat flux: 92 – 1009 kW/m²	- For $\tau > \tau_c$: Wall temperature under oscillatory flow is higher than steady-state conditions. - For $\tau < \tau_c$: Opposite behavior is observed. - Flow oscillations deteriorate boiling heat transfer when 1.04 $\leq$ s $\leq$ 10.6 s. - Fp is lower than 1, meaning critical heat flux-(CHF) is pre-triggered by oscillations. - For P $\leq$ 3 MPa, oscillation effects are minimal, and at higher P, void fraction increases, which reduces the boiling crisis impact. -Higher average mass velocity Gav leads to lower Fp, especially for short oscillation periods (1.04 – 2.1 s).
[50]	**Analytical**	Parallel plate channel with variable wall heat flux.	- 20 inches	- Re $\approx$ 2000	- Wall temperature response depends on both heat flux variation and flow velocity oscillations. -Transient heat transfer equations were developed with varying heat flux along the channel length. - For slow heat flux changes, simplified models with a constant heat transfer coefficient provide good agreement (±10-15%). -For fast transients, differences up to 25% were observed compared to constant Nu models.

[51]	**Numerical**	Circular cylinder (Bluff body) in rotational oscillation	-The spanwise length was L_z= 2D -the streamwise and crosswise dimensions L_x X L_y = 25D X 20D	-Rotational Frequency Ratio: 0, 1, 2.5, 4 - A: 1, 2 - Re= 1.4×10^5	- At f = 1, Nu increases by ~10% (consistent with lock-on effects in low-Re regimes). - Higher frequencies (f = 2.5, 4) lead to a decrease in Nu due to reduced coherent structures - Large-scale coherent structures enhance heat transfer at the rear surface. - Rotary oscillation reduces temperature fluctuations and evens out heat transfer distribution. -The drag coefficient (Cd) drops significantly at f = 2.5, A= 2 (compared to f = 1).
[52]	**Numerical**	- Heated circular cylinder in transverse oscillation. -Placed inside a channel	- height (h): 10d - inlet length 10d - outlet length: 30d - Blockage Ratio (d/h): 0.1	-Oscillation Frequency (Fc): 0.1 -0.4 -Oscillation Velocity Ratio (V_m/ V_0): 0.25 - 1.0	- Nusselt Number (Nu) increased by 10-22% compared to stationary cases. - For Fc = 0.2, heat transfer is maximized due to vortex shedding synchronization -For Fc = 0.1 or 0.4, less improvement in heat transfer was observed. -V_m = 1.0 → Nu increased by ~21.9% Re = 500 → Nu increased by ~28.7% -At lock-in regime (Fc = 0.2), the Nusselt number is maximized.
[53]	**Numerical**	-Wavy Mini-Channel -Sinusoidal Wall Geometry	- Length (Lt): 21 mm - Hydraulic Diameter (H): 1 mm - Wavy Amplitude (Aw): 0.2 mm - The wavelength (λ): 1 mm	- Ao: 0.5, 0.8, 1.0 - $1 \leq St \leq 10$ - Re=100	- Nu increases with nanoparticle volume fraction. - Heat transfer is maximized at St = 2 (low frequency). - Higher Ao increases heat transfer due to stronger convective mixing. - For Ao = 1.0, heat transfer enhancement reaches ~28%. - Heat Transfer Performance: increases with Ao and φ, but decreases with increasing St beyond St = 4
[54]	**Numerical**	-Rectangular channel with periodically mounted obstacles on both upper and lower walls -Obstacles are heated	- Channel Height: H - Obstacle Height (h): 0.25 H - Obstacle Width (w): 0.25 H - Obstacle Spacing (L): 1.0 H	- Re=50-1000	-Overall Nusselt Number (Nu) increases with Re. - Nu increase from Re = 50 to Re = 500: 123.1% -Nu increase from Re = 500 to Re = 1000: 48.5% - Max Nu enhancement was observed near obstacle corners due to vortex interaction. -Transition to unsteady flow observed at Re ≈ 500. -Using obstacles on both walls increases Nu by up to 141% at Re = 1000 compared to obstacles on one wall. The friction factor increases by a factor of ~19 at Re = 1000.
[55]	**Numerical**	Spherical Corrugated Helical Tube	- Helix Diameter: 0.33 m - Tube Diameter: 0.02 m -Coil Pitch (Pc): 0.04 m -Corrugation Height (e): 0.026 m -Corrugation Pitch (H): 0.04 m	- Dean Number (De): 2936 - $0 \leq Wo \leq 50$ - Amplitude: 0.25 – 0.75 - Re=9940 – 19880	- Compared to a steady flow, the average local Nusselt number (Nu) increases by up to 38.5%. - Overall thermal performance improves by 13% at De = 2936, Wo = 35, $\bar{A}$ = 0.5. - For Wo < 35, increasing Wo enhances heat transfer. -For Wo > 35, thermal performance decreases due to excessive turbulence dissipation.
[56]	**Numerical**	-Spirally Corrugated Tube with a two-start spiral configuration -Comparison between smooth and corrugated tubes	-Tube Length (L): 400 mm - Hydraulic Diameter (d): 13.3 mm - Corrugation Depth (e): 3 mm - Spiral Pitch (s): 40 mm	- ω: 20π rad/s - f: 10 Hz - Re_{max} = 4608 - Re_s=350	-Average Heat Absorption (Q) in Spirally Corrugated Tube = 1.36 times that of Smooth Tube -Heat Absorption Increase: 561 W more than the smooth tube - Outlet Temperature Increase: -Smooth Tube: 205 K increase -Corrugated Tube: 365 K increase -Spiral motion intensifies turbulence and boundary layer disruption -Pressure drop in corrugated tube = ~430 Pa higher than smooth tube
[57]	**Numerical**	Wavy-walled tube heat exchanger	- Tube Wavelength (λ): 25 mm - Maximum Diameter (D_{max}): 16 mm - Minimum Diameter (D_{min}): 9 mm	- $0.2 \leq f \leq 2$ - A: 0.2 - 2.0 m - Re=100-600	-Nusselt Number (Nu) increased by 76 – 124% compared to steady flow. - Maximum Nu enhancement at f_T = 1.0 Hz and A = 1.0 m. -For f_T > 1.5 Hz, Nu stabilizes due to turbulence dissipation effects. -For A = 2.0 m and f_T = 2.0 Hz, the pressure drop is 146.8% higher than a steady flow. - At moderate fT (1.0 Hz), pressure fluctuations remain stable, balancing heat transfer and resistance. -Field Synergy Number (Fc) decreases as Reynolds number (Re) increases. -Best synergy achieved at pulsation frequency f_T = 1.0 Hz and A = 1.0 m.

4. Sinusoidal wavy surfaces

Wavy tubes are a class of periodic surfaces characterized by sinusoidal or corrugated wall profiles along the tube length. These geometries are widely employed in heat exchangers to enhance heat transfer performance without significantly increasing the device size. The periodic surface fluctuations force the flow to continuously accelerate and decelerate, inducing secondary vortices and enhancing fluid mixing. This disruption of the thermal and velocity boundary layers enhances convective heat transfer compared with smooth tubes. The hydrodynamic behaviour in wavy tubes is highly dependent on the wavelength and amplitude of the waviness. Shorter wavelengths and larger amplitudes promote stronger vortex formation and higher heat transfer, but they also introduce higher pressure drops due to flow separation and reattachment cycles. Therefore, wavy tubes offer a trade-off between enhanced heat transfer and compromised hydraulic performance. These effects are particularly advantageous under oscillatory flow conditions, where convective heat-transfer efficiency can be further increased by combining geometric undulations with flow pulsations. Many studies have employed experimental and numerical methods to investigate the effects of sinusoidal geometry in various heat exchanger systems because of its potential benefits.

G. Russ and H. Beer [58] studied fully developed flow and heat transfer in a sinusoidal wavy pipe with periodically converging-diverging cross-section over a total length of 11 wavelengths. The study focuses on enhancing convective transport across a range of Reynolds numbers (Re), from laminar to turbulent flow. The findings showed that Nusselt and Sherwood values were strongly influenced by vortex interactions, flow separation, and turbulent structures, with maxima occurring near reattachment points. Convective transport is improved with increasing wave amplitude (λ) and reducing wavelength (γ_h), but the pressure drop is increased, as established in the study. The Nusselt number exhibits local maxima near reattachment points for laminar flow (Re = 300), but overall heat transfer remains close to that of a smooth pipe. Shear-induced turbulence and flow substantially increase the Nusselt number in transitional and turbulent flows (Re = 2000–8000). Fully developed turbulent flow increases heat transfer by a factor of 1.5–2 relative to a straight pipe.

G.Russ and H. Beer[59] experimentally investigated the heat transfer and flow field in a sinusoidally wavy pipe of total length 1980 mm, containing 10.5 waves, a wavelength of 188.5 mm, and a wave amplitude of 0.01 mm. The results showed that, for laminar flow (Re = 300), the Nusselt number was lower than that in a smooth pipe due to the insulating effect of recirculating bubbles. However, for transitional and turbulent flow (Re > 2000), the Nusselt number increases significantly because of flow separation, reattachment, and shear-layer instabilities, reaching values up to 2.5 times those in a smooth pipe at the highest Reynolds numbers. This enhancement is associated with an increased pressure drop, indicating a trade-off between heat transfer and friction losses**.** Jang and Yan [60] used a marching finite-difference approach to numerically investigate the transport of mass and heat from mixed convection down a vertical wavy surface. According to the study, the temperature, velocity, and concentration distributions exhibit periodic variations along the wavy surface, with the fluctuations decreasing downstream. Higher amplitude–wavelength ratios produce greater velocity changes but lower rates of heat and mass transfer, whereas increasing the buoyancy ratio and Richardson number enhances heat and mass transfer. The results confirm that mixed convection exhibits two distinct harmonics: forced convection is more prevalent near the leading edge, whereas free convection becomes increasingly essential downstream. Harikrishnan and Tiwari [61] analysed the effects of skewness on heat transfer flow characteristics in wavy channels, as shown in Figure 10. The simulations cover a range of Reynolds numbers (Re = 2000–4000) and a range of wave amplitudes.

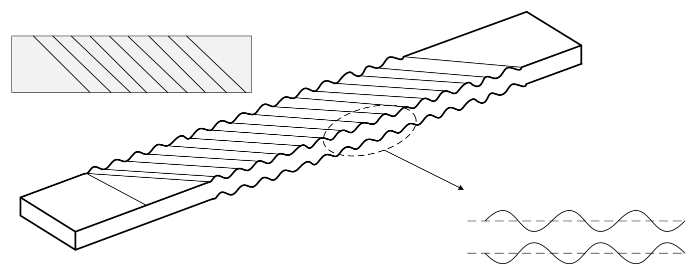

Figure 10. Top and isometric views of the skewed wavy channel. [61]

The findings indicate that skewness enhances secondary flow by increasing the Nusselt number and the friction factor (f) until the skewness angle ϕ reaches 30°–35°, after which both decrease. The performance evaluation criterion (PEC) is recorded at a wave-amplitude-to-channel-height ratio (a/H) = 0.2 and at a phase angle (ϕ) of 45°. Heat transmission, not viscous effects, predominates even if entropy formation increases with skewness. Ramgadia and Saha [62] used a finite volume method to quantitatively study fully developed flow and heat transport in a wavy channel. The findings indicate that as H_{min}/H_{max} increases, the critical Reynolds number for flow unsteadiness lowers. Model M2 (H_{min}/H_{max} = 0.2) has the highest Nusselt number (Nu = 9.572) and Performance Evaluation Criterion (PEC = 1.765), as shown in Table 4. The trade-off between pressure drop and heat transfer enhancement is illustrated by the PEC values given in Table 4. Configurations with PEC values greater than unity, which indicate a net thermal-hydraulic benefit, suggest promising design alternatives. Differences in outcomes across situations further highlight the role of geometry in performance optimization. In addition to improving heat transfer, higher waviness also raises the friction factor (f = 7.633 for H_{min}/H_{max} = 0.1). The study identifies the optimal shapes that maximize thermal performance and confirms that unsteady flow significantly enhances heat transfer.

Table 4. Dimensionless number comparison at Reynolds number of 600.[62]

Model	Friction factor $f\ (f/f_o)$	Nusselt number $Nu(Nu/Nu_o)$	PEC	Strouhal, St
M_1	0.305 (7.633)	8.435 (2.237)	1.136	0.366
M_2	0.119 (2.978)	9.572 (2.539)	1.765	0.320
M_3	0.126 (3.153)	8.022 (2.128)	1.451	0.171
M_4	0.096 (2.400)	7.760 (2.058)	1.537	0.305
M_5	0.068 (1.704)	5.615 (1.489)	1.247	0.458

Chang et al. [63] investigated heat transport and pressure drop in furrowed channels with transverse and skewed sinusoidal wavy walls experimentally across a range of Reynolds numbers from 1000 to 30,000. The findings showed that compared to smooth channels, skewed waviness enhances secondary flows, increasing the Nusselt number (Nu) and the friction factor (f) by factors of 3.98-4.2 and 5.36-10.5, respectively. Skewed waves exhibit the maximum value of the performance evaluation criterion (PEC = 4.6) at Re = 2000. Skewed wavy walls offer a similar increase in heat transfer to V-ribs but with lower pressure-drop penalties, according to empirical correlations calculated for Nu and f. Guzmán et al. [64] employed direct numerical simulations to investigate how bifurcations in flow within asymmetric wavy wall channels can enhance heat transfer. One Hopf bifurcation results in a periodic flow at aspect ratios of 0.25 and 0.5, and two Hopf bifurcations result in the flow transitioning from laminar to periodic to quasi-periodic at an aspect ratio of 0.375. The Nusselt number increases as the Reynolds number increases, with the most significant increase occurring at an aspect ratio of 0.5. According to the findings, substantial heat transfer enhancement can be achieved by operating in the transitional Reynolds-number regime, without the high power consumption associated with the turbulent flow regime.

Bai et al.[65] used large eddy simulations (LES) at $Re = 3.0 \times 10^3$ and $Pr = 0.7$ to study the near wake flow and forced convection heat transfer around a sinusoidal wavy cylinder. According to the results, wavy cylinder significantly alters the wake flow, affecting Reynolds stresses and heat flux distributions. Recirculation bubble dynamics and coherent spanwise vortices are intimately related to heat transfer performance. The wavy cylinders with $\lambda = 1.89$ and 6.06 exhibit reduced fluid forces (reduced drag and lift fluctuations) and lower heat transfer efficiency (~11% less than the smooth cylinder). The results indicate the optimal balance between enhancing heat transfer and improving aerodynamic performance in engineering applications. Yi-Gao Lv et al. [66] numerically investigated the thermal-hydraulic performance of hybrid wavy channels in a printed circuit heat exchanger (PCHE) used as a supercritical CO_2 (S-CO_2) precooler.

Three hybrid channel design types, A, B, and C, which combined straight and sinusoidal wavy sections in various configurations, were examined According to the study, the type-C channel, which has the wavy portion in the low-temperature area, performed best overall, reducing pressure drop by up to 23% and increasing the local heat transfer coefficient by 1.56 $kW/m^2{\cdot}K$ compared with the straight channel. The study also established that shorter wavelengths and larger wave angles further enhance performance. In low-temperature areas, gravity had a minor impact on heat transmission and hydraulic performance. These findings support the effectiveness of techniques that match thermophysical properties to enhance partitioned heat transfer in the design of efficient S-CO_2 precoolers.

Ahmed et al.[67] investigated laminar copper–water nanofluid flow and heat transport in a two-dimensional wavy channel numerically using the finite difference method. They examined the effects of wavelength (L), wavy-wall amplitude (A), Reynolds number (100–800), and nanoparticle volume fraction (0–5%). According to the results, increasing the nanoparticle volume percentage can increase the average Nusselt number by up to 90%, whereas the skin-friction coefficient increases only slightly. Thermal performance is significantly enhanced by increased wave amplitude and Reynolds number, while the wavelength has a lesser impact. The results validate that heat exchanger efficiency can be effectively enhanced through the use of nanofluids and the geometric optimization of wavy channels. Ahmadpoura and Abadi [68] investigated the thermal-hydraulic performance of turbulent gas-liquid multiphase flows in vertical sinusoidal wavy channels, both with and without phase change, using numerical methods. The two scenarios examined are adiabatic air-water flow and condensing R134a flow, simulated using the Volume of Fluid (VOF) method and the SST turbulence model. The wavelength, amplitude, and phase shift angles between sidewalls (0°, 90°, and 180°) of the wavy channels are examined for the condensing R134a scenario. The findings indicate that compared with straight channels, heat transfer coefficients can increase by as much as 40% and pressure-drop penalties can be up to six times greater. Only at low mass flux ($G = 50\ kg/m^2{\cdot}s$) does the Performance Evaluation Criterion (PEC) increase, especially for a 180° phase shift. It suggests that wavy channels are best suited for condensation applications at low flow rates.

To achieve better thermal-hydraulic performance, recent developments have integrated oscillatory flow with wavy microchannel geometry. A biomimetic bark-shaped microchannel heat sink was developed by Daba et al.[69], who demonstrated through CFD and testing that pulsing flow at 2 Hz and Re = 2000 decreased thermal resistance by approximately 40% and the maximum wall temperature by around 35 K compared to straight channels. The bark-like design yielded a performance evaluation criterion(PECR)of 2.68. It increased the surface area by more than 25%, demonstrating that geometry-induced mixing, in conjunction with flow pulsations, can significantly enhance overall efficiency.

In addition to these developments, recent studies have highlighted the influence of nanoparticle characteristics on heat transfer in wavy geometries. Nguyen et al.[70] examined the impact of nanoparticle form in their numerical analysis of forced convection of a CuO–

water nanofluid in a sinusoidal channel with obstructions. The four morphologies (spherical, brick, cylindrical, and platelet) were examined across obstacle height ratios (HR = 0–0.5), wavelength ratios (λ/H = 0.15–0.2), and Reynolds numbers (Re = 100–400). The findings demonstrated that, compared with spherical particles, platelet-shaped nanoparticles produced the greatest increase in heat transfer rates, amounting to more than 55%. Larger wavelength and obstacle-height ratios enhanced convective heat transfer and intensified vortices, while an increased Reynolds number raised the Nusselt number. To account for these combined effects, a correlation for Nu was proposed. Mousavi et al. [71] numerically investigated ferrofluid flow (4 vol% Fe_3O_4, 10 nm) in a sinusoidal channel under a transverse magnetic field. They discovered that the magnetic field (Mn up to 3.31×10^7) increased skin friction by more than 600%, improved eddy formation, and increased heat transfer by more than 200% at Re = 50. According to the study, cooling efficacy is substantially enhanced when sinusoidal geometries and magnetic fields are applied, especially at low Reynolds numbers.

5. Corrugated tubes and channels

Apart from sinusoidal shapes, corrugated tubes and channels have garnered significant interest in recent years due to their compactness and thermal performance. The corrugation periodically deforms the wall (usually in the form of ridges or grooves), disturbs the boundary layer, increases fluid mixing, and encourages the development of secondary flows. These effects maintain a relatively small increase in pressure drop while enhancing convective heat transfer rates. Compact heat exchangers, solar thermal collectors, and refrigeration systems, which frequently require heat transfer enhancement and address spatial constraints, often assume a corrugated form. Corrugated forms are appealing because they can be used in both single-phase and multiphase flow, offering a reasonable trade-off between efficiency and fabricability compared with smooth or straight tubes.

Sun and Zeng [72] employed the same constraints, including mass flow rate, pumping power, and pressure drop, in their study. This study presents an experimental and numerical investigation of heat transfer under turbulent flow conditions in three types of corrugated tubes compared with plain tubes. Under uniform heat flux boundary conditions, the study uses air as the working fluid and considers a Reynolds number range of 4,000 to 100,000. The findings indicate that corrugated tubes can increase the mean Nusselt number by up to 50%. Greater heat transfer results from the combined effect of higher velocity and a larger temperature gradient, which yields a more than 50% increase in the convective contribution and reduces synergy angles by approximately 1-2°. Economically, utilizing corrugated tubes in ground-source heat pump systems could reduce the cost index from \$0.1 to \$0.08/kJ, indicating significant cost and energy savings. Based on the findings, corrugated tubes have substantial potential for the efficient design of thermal systems. Andrade et al. [73] investigated the heat transfer and pressure drop behaviour of internal flow in corrugated tubes under laminar, transitional, and turbulent regimes, experimentally utilising water as the working fluid. The Nusselt number increased by up to 4.7 times (p = 6 mm) and 3.8 times (p = 12 mm) relative to the smooth tube, indicating that corrugated tubes permit heat transfer, particularly in the transitional regime. Corrugated tubes exhibited a smoother laminar-to-turbulent transition and a higher friction factor. According to Colburn's J-factor analysis, corrugated tubes perform better in the transitional flow regime or when thermohydraulic performance is optimized.

Bayareh and Nourbakhsh[74] numerically investigated seven corrugated tube geometries (smooth, convex, concave, and combined) with three nanofluids (CuO–water, ZnO–water, and SiO_2–water at 3% volume fraction) using ANSYS Fluent and the standard k–ε turbulence model (Re = 10,000–17,500). Compared with the smooth tube, the convex–concave design performed best thermally and produced the greatest enhancement of the Nusselt number. The CuO–water nanofluid demonstrated the best thermal behaviour among the nanofluids due to copper's superior thermal conductivity, albeit with a greater pressure drop. While Bayareh and Nourbakhsh demonstrated that corrugated geometries combined with nanofluids (CuO, ZnO, SiO_2) enhance heat transfer, more recent studies extended this approach by integrating additional mechanisms. For example, FeO_4/H_2O nanofluid in wavy tubes with helical ribs was examined numerically by Varkaneh et al.[75]. The results demonstrated that applying stronger fields, lowering rib pitch, and raising rib height significantly improved thermal performance. The best instance, achieved at Re = 4,000 with B = 600 G, demonstrated a significant improvement at low Reynolds numbers, reaching a maximum PEC of ≈3.3. These results suggest that corrugation can enhance heat transfer by working in conjunction with nanofluids and magnetohydrodynamic processes.

Al-Obaidi [76] investigated the flow behaviour, pressure drop, and heat transfer enhancement in smooth and circular corrugated tubes with ring radii of 0.375 mm, 0.5 mm, and 1 mm using numerical simulations. Using a uniform heat flux of 800 W/m^2, the analyses were carried out for Reynolds numbers ranging from 1,500 to 24,000 and flow rates ranging from 0.56 to 8.33 L/min. The results showed that at the minimum flow rate (0.56 L/min), the 1 mm corrugated ring achieved the greatest improvement in heat transfer (26.48%); the 0.5 mm and 0.375 mm rings showed improvements of 19.43% and 15.26%, respectively. Increasing the corrugation radius increases turbulence, secondary flows, and mixing, thereby improving heat transfer but increasing pressure loss. Córcoles et al.[77] investigated the pressure drop in a double pipe heat exchanger with nine inner tubes, which include eight spirally corrugated and one smooth, spiral flow regime under turbulent conditions as described by Reynolds numbers of 25,000–50,000. With the highest corrugation height (H/D = 0.05) and the lowest pitch (P/D = 0.682), this case exhibited the highest pressure drop: the inner and annular sides recorded pressure drops 4.15 and 1.27 times higher than those of the smooth tube, respectively. Case 9 (with H/D = 0.041 and P/D = 0.682) had the highest heat transfer rate (Q) and the highest overall heat transfer coefficient (U = 3251.4 $W/m^2 \cdot °C$), yielding a 29% increase in the number of transfer units (NTU) and a 23% increase in efficiency over the smooth tube. The performance evaluation criterion (PEC) indicated a good balance between improved heat transfer and pressure drop, reaching a value of up to 1.12.

Artemov et al. [78] numerically simulated the flow of liquid nitrogen in corrugated annular tubes with high-temperature superconducting (HTS) cables. The simulation investigated the impact of varying the corrugation pitch-to-hydraulic-diameter ratio (p/de) from 0.06 to 0.54 and the corrugation depth-to-hydraulic-diameter ratio (h/de) from 0.06 to 0.3, for Reynolds numbers up to 30,000. The results showed that with a worst-case deviation of less than 30%, the k–ω models and the LVEL (Local Velocity and Eddy Length) turbulence model best matched the experimental data. The pressure loss in the investigated geometries was due to wall shear stress in only about 5%; pressure gradients in near-separation regions were primarily responsible. Additionally, compared with a concentric installation, the eccentric positioning of the HTS cable (e = 1) resulted in a 20% reduction in the friction factor.

Kurtulmuş and Besir Sahin [3] provided a comprehensive evaluation of flow and heat transfer behaviour in corrugated channels of various shapes, including trapezoidal, arc, rectangular, sinusoidal, and sharp geometries. It aggregates the results of more than 70 research publications and considers both active (e.g., flow pulsation) and passive (e.g., geometrical modifications and nanofluids) methods for enhancement. One significant finding is that sinusoidal channels exhibit up to a 50% improvement at a 10% volume fraction of copper nanoparticles. In contrast, sharp corrugated channels can improve heat transfer by a factor of up to 3.2, albeit at the cost of a very high pressure drop. For square channels, an amplitude-to-channel height ratio of 0.3 (2a/H) yields a 30% improvement at a Reynolds number (Re) of 3000.

Furthermore, corrugated geometries and oscillatory flow can double the thermal performance while requiring pumping power that is two orders of magnitude lower. To assist engineers in designing effective heat exchangers, this paper presents optimal designs and operating conditions that maximize the performance evaluation criterion (PEC), which typically exceeds 1.0 at moderate Reynolds numbers. Figure 11 presents the results of several studies [[79],[62],[80],[81],[82],[83],[84] and [85]] on sinusoidal and corrugated channels. The performance evaluation criterion (PEC), which reflects the quantitative balance between heat transfer enhancement and pressure-drop penalties, generally exceeds unity; it increases with Reynolds number up to a specific limit and then declines. This comparison highlights the overall thermal–hydrodynamic performance trends for various periodic-surface configurations. Table 5 lists the most commonly used periodic surfaces from previous investigations, along with their geometric parameters and thermal enhancements.

In addition, Manh et al. [86] used the Homotopy Perturbation Method (HPM), which was verified against a 4th-order Runge–Kutta (RK4) scheme, to examine the hydrodynamic behavior of nanofluid flow between non-parallel plates when subjected to a magnetic field. The findings indicated that while higher Ha increased boundary layer thickness, increasing ϕ and Re decreased it. Furthermore, centerline velocity was considerably reduced with increasing α (down to 40% at α = 10°). The results demonstrate how magnetic fields and nanoparticles work together to improve thermal-hydraulic performance in non-parallel geometries and to control the flow structure. Recent research has also examined nanofluid flows in magnetic fields and demonstrated their potential to control recirculation and enhance heat transfer. Manh et al.[87] used CFD with the FVM and SIMPLEC algorithm to numerically investigate nanofluid flow along a backwards-facing step subjected to a non-uniform magnetic field. At Reynolds numbers Re = 50–150, a ferrofluid with 4 vol% Fe_3O_4 nanoparticles (10 nm) in water was investigated under a constant wall heat flux (10,000 $W{\cdot}m^{-2}{\cdot}K^{-1}$). The findings showed that raising the magnetic number (Mn = 1.37×10^6–7.47×10^6) improved heat transfer and recirculation zones, with the local Nusselt number increasing by up to 300% compared with the non-magnetic scenario. Multiple magnetic sources were also added, increasing circulation and further enhancing thermal performance. These results indicate that in separated-flow geometries, time-varying magnetic fields can significantly enhance heat transfer and regulate nanofluid flow. Barzegar Gerdroodbary et al. [88] numerically studied ferrofluid flow in a screw heat exchanger with 4 vol% Fe_3O_4 nanoparticles under a non-uniform magnetic field, They demonstrated that while screw diameter(6–10 mm)and magnetic intensity(Mn ≈ 8.55×10^7) both improved heat transmission but increased skin friction, Reynolds number(Re = 3000–5000)had the greatest effect on thermal performance.

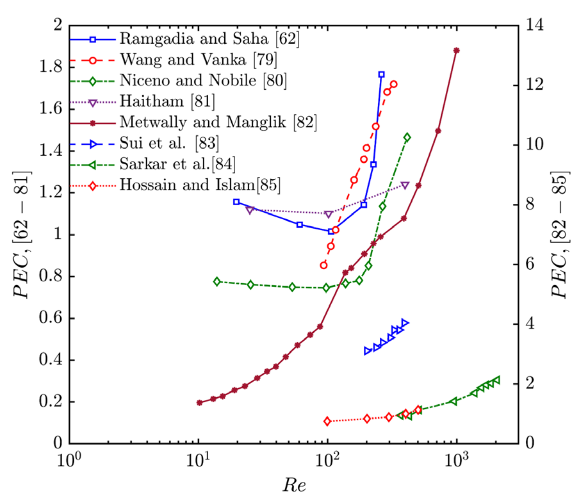

Figure 11. Variation of the PEC with Reynolds number for different periodic-surface geometries

Table 5. Summary of previous studies with sinusoidal wavy and corrugated tubes and channels

Ref	Geometry	Length (L)	Wavelength (P)	Wave amp.(A)	Re	Thermal Enhancement
[58]	Sinusoidal wavy pipe, Periodically converging-diverging pipe	11 sinusoidal waves in the pipe for fully developed flow.	γp= 3.14 γp =6.28 γp =7.83 These values are dimensionless, so the actual physical values depend on the mean radius, r_m p= γp*r_m	γA =0.26 γA =0.33 γA =0.40 A= γA*r_m	-Laminar flow: Reynolds number based on the mean diameter, Re_{dm}=300 -Transitional flow: Starts around Re_{dm}=600 to 2000 -Turbulent flow: Up to Re_{dm}=8000	- The enhancement compared to a straight pipe is minor under laminar conditions. - The mean Sherwood number (mass transfer) and Nusselt number (heat transfer) both increase considerably with the increase in Reynolds number and larger amplitude-to-wavelength ratios. -The enhancement could reach up to several times the values in a straight pipe, especially near separation and reattachment points, where shear-induced turbulence is strongest.
[59]	Sinusoidal wavy pipe (periodically converging-diverging cross-section).	-Total length: 1980 mm - Number of waves: 10.5 sinusoidal waves.	0.1885 m.	0.01 m.	-Laminar: Re_{dm}≤400 -Transitional: 400<Re_{dm} <2000 -Turbulent: Redm>2000	At Re=8000 -The mean Nusselt number per wavelength is approximately 1.5 to 2 times higher than in a smooth straight pipe. - Local peaks (at reattachment points) can be up to 3-4 times higher than the minimum values within a wave. -A shorter wavelength and higher amplitude further enhance the Nusselt number by increasing turbulence production.
[60]	Vertical wavy surface $y=r(x)=a \sin^2(\pi x/L)$	Semi-infinite	Variable with a/L = 0 to 0.1	5% - 10% of P	Variable (focus is on Ri = 0 to 10)	Nu increases with buoyancy ratio and Richardson number, but decreases with increasing amplitude-to-wavelength ratio.
[61]	Skewed wavy channel (a sinusoidal wavy channel where the waves are inclined at a skewness angle ϕ to the spanwise direction).	-total streamwise length: L=30H -Entry length: L1=5H - Exit length: L_{ex}=13.5H	1.5H	0.1H, 0.2H, 0.3H	2000 ≤ Re ≤ 4000	-Up to ~15% higher at optimal skewness φ = 35° (compared to unskewed case). -The highest PEC for φ = 45° and a = 0.2H, indicating the best balance between heat transfer enhancement and friction penalty.
[62]	Sinusoidal wavy channel. $y=2a\sin^2(\pi x/L)$	L	L-fixed length	L/A -Varied through the parameter H_{min}/H_{max}, from 0.1 to 0.5	25 ≤ Re ≤ 600	-Up to 2.54x over the parallel-plate channel. -H_{min}/H_{max}=0.2 (highest heat transfer and PEC)
[63]	Furrowed channel with transverse and skewed sinusoidal wavy walls	194 mm (about 16 wavelengths).	-p=12 mm. -Channel width:54 mm. -Channel height:13.5 mm.	2.4 mm.	1000 ≤ Re ≤ 30000	-Up to 4.2x Dittus–Boelter for skewed walls (highest). -In laminar flow (1000 < Re < 2000): -Nu/Nu1 = 5 to 8.8 (transverse). -Nu/Nu1 = 5.4 to 11.3 (skewed). -In turbulent flow (5000 < Re < 30000): -Nu/Nu1 = 3.45 to 3.71 (transverse). -Nu/Nu1 = 3.98 to 4.2 (skewed).
[64]	Asymmetric wavy wall channel(Sinusoidal)	12 × wavelength = 12×4.6666×= 56.0 (approx.)	p= 4.6666	A=4.333	-r = 0.25: Re = 40 to 300 -r = 0.375: Re = 2 to 260 -r = 0.5: Re = 8 to 130	Up to 5-6 times increase in transitional flow (compared to laminar)
[65]	Sinusoidal wavy cylinder.	Depends on wavelength (between ~3.79 and 12.12 D_m), where D_m is a normalization parameter that refers to the mean diameter.	1.89D_m,3.79D_m,6.06D_m	A=0.152D_m	3000	Slight reduction (up to ~11% lower than a smooth cylinder)

[66]	Hybrid wavy channels. Straight channels and sinusoidal wavy channels.	L=442.8 mm	- p=24.6 mm (in the baseline case, Other cases studied include: p=12.3 mm and P=18mm	2 mm.	7500 ≤ Re ≤ 22500	Type-C (when the wavy section is placed in the low-temperature region (near the outlet): 1.56 kW/m²·K increment; 2.6x higher than Type-A (wavy section is placed in the high-temperature region (near the inlet).; 23% lower pressure drop than Type-A
[67]	Two parallel sinusoidal wavy plates.	At P=44, L=344mm At P=56, L=416mm At P=72, L=512mm	-p=(44, 56, 72)mm.	0, 0.1H, 0.2H, 0.3H (where H is the half-channel height = 20 mm). So, A=(2, 4, 6)mm	100 ≤ Re ≤ 800	-Up to 90% higher than a smooth channel with water. -The enhancement increases with a higher Reynolds number. -Larger amplitude. -Higher nanoparticle volume fraction.
[68]	Vertical sinusoidal wavy channel.	1m	67.2 mm	5.76 mm	Re ≈ 5470 Re ≈ 10940 Re ≈ 21880	Up to 40% enhancement for low mass flux; lower thermal performance for higher mass flux due to pressure drop
[72]	corrugated tube	Tube1=954mm Tube2=1129mm Tube3=1242mm	Tube1=22mm Tube2=28mm Tube3=34mm	Tube1=1.5mm Tube2=1.5mm Tube3=2.5mm	4000 ≤ Re ≤ 100000	-The Nusselt number of the corrugated tubes is increased by approximately 50% compared to plain tubes., This enhancement is mainly due to the improved synergy between velocity and temperature gradient caused by the corrugated shape.
[73]	Helically corrugated tube (spiral corrugation along the tube length).	-Heating length: 380 mm -Developing section length: 820 mm	Tube p6: 6 mm. Tube p12: 12 mm	0.6 mm (for both corrugated tubes)	429 ≤ Re ≤ 6212	-Maximum Nusselt number enhancement: up to 4.7 times for P6 and 3.8 times for P12, compared to smooth tubes. -The best enhancement occurs around Re = 2000. -The friction factor increases significantly due to corrugation. Average augmentation: 11.3 times for P6 and 4.8 times for P12 in laminar flow.
[76]	3D circular corrugated tube	1920 mm	NA	0.375, 0.5, 1 mm.	1500 ≤ Re ≤ 24000	-Best heat transfer enhancement occurs at a low flow rate (0.56 L/min) with the largest corrugated ring (1 mm radius). - 1 mm ring: 26.48% enhancement - 0.5 mm ring: 19.43% enhancement - 0.375 mm ring: 15.26% enhancement
[77]	Double-pipe heat exchanger with inner corrugated tubes	2.9 m	p=15, 20, and 25 mm	0.7, 0.9, and 1.1 mm	25,000 and 50,000	-The heat transfer rate increased between 12% and 23% when compared to a smooth tube. - The NTU (Number of Transfer Units) increased by 29% in the best-performing case. -The highest enhancement was observed in Case 9, which had a 23% increase in heat exchanger efficiency
[78]	Corrugated annular channel with a transversally corrugated outer wall.		6.5 mm	3 mm	up to 30,000	-The friction factor increased with increasing corrugation depth and pitch ratio. - Eccentric placement of the cable reduced the friction factor by 20% compared to a concentric arrangement. - The pressure drop prediction in cryogenic channels was improved by up to 30% using the selected turbulence models
[89]	Asymmetric wavy wall channel	Periodic (1 wavelength at a time)		a=0.5, b=0.4(examples)		-The Brinkman number (Br) increased the temperature values. -The thermal slip parameter (f) increased the temperature. -The Grashof number (Gr) also increased the temperature.
[90]	Wavy elliptic cylinder.	No fixed total length is specified, as the study focuses on periodic behaviour along the span. λ=1.0Lm, x to 8.0Lm,x	1.0≤≤ 8.0	a = 0.1 Lm,x	100	Up to ~10% compared to the smooth elliptic cylinder at optimal aspect ratio and wavelength. Enhancement reduces as the cylinder becomes more streamlined (lower AR).

[91]	Sinusoidal wavy channel in a Printed Circuit Heat Exchanger (PCHE).	(covering 10 full wavelengths): L=246 mm	15.78 mm	0.62 mm	1800 ≤ Re ≤ 13000	-CO_2-He: up to 396% increase -CO_2-Kr, and CO_2-Xe: up to 71% and 80% reduction, respectively. -Pure CO_2 gives the highest thermal-hydraulic performance (η), but CO_2-Xe shows acceptable performance with thermodynamic cycle advantages due to its impact on critical temperature and pressure.
[92]	Wavy-walled tube in a shell and tube heat exchanger.	-Tube length: 560 mm -Overall heat exchanger length (L) = 760 mm	25 mm	3.5 mm	500 ≤ Re ≤ 4000	-Nu: Maximum increase of 9.67% -Pressure drop: Decreases by 5.25% (for the wavy-walled tube compared to the straight-walled tube)
[93]	Wavy-walled tube (corrugated tube with smooth periodic waves along the length).	1.0 m	0.025 m	0.001 m	100 ≤ Re ≤ 500	Maximum heat transfer enhancement (Eh) reaches 36.2% higher than using pulsating flow alone.
[94]	Corrugated circular pipe (3D) with variable distances between these rings, different angles of the corrugated arc ring (CARA)	1m	implicitly defined as the spacing between corrugation rings = (2,4, and 6)mm	related to the corrugation angular extent. CARA: 10°, 20°, and 30°	4000 to 12,000.	-The Nusselt number enhancement (Nu/Nu_0) compared to a smooth pipe ranges from 1.02 to 2.9 times higher, depending on the configuration. -(Distance Between Arc Rings)DBAR = 2 mm, (Corrugated Arc Ring Angle)CARA = 30°, and arc ring angle around the Pipe (ARAAP) = 240° showed the highest heat transfer improvement. -For ARAAP (angle around the pipe)=240:Nu increased by 11.4% to 38% -Friction factor increases by 1.2 to 2.9 times compared to smooth pipes
[95]	-Symmetric sinusoidal wavy-walled channel.	The test section contains 14 furrows, meaning: 14×14 mm=196 mm	14 mm.	3.5 mm	30 ≤ Re ≤ 300	- Sherwood number (Sh) is significantly enhanced by combining flow separation and oscillatory flow. -The enhancement factor increases with oscillatory fraction and Reynolds number. -The enhancement formula is: Shpp = Shs + Sho

Table 6. Previous studies of periodic surface configurations

Ref	Configurations	Ref	Configurations
[58]	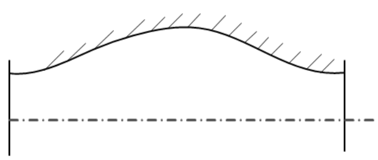	[76]	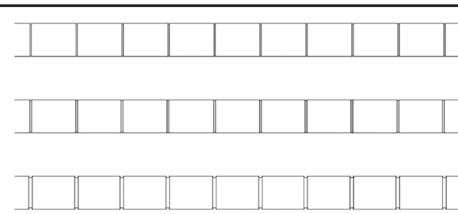
[61]	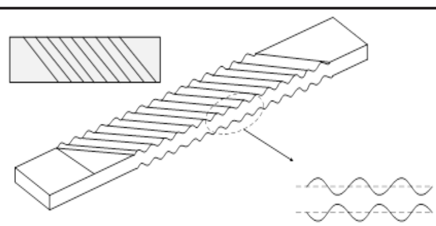	[77]	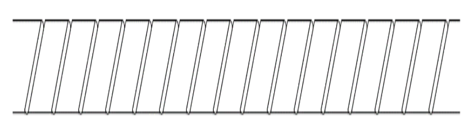

[64]	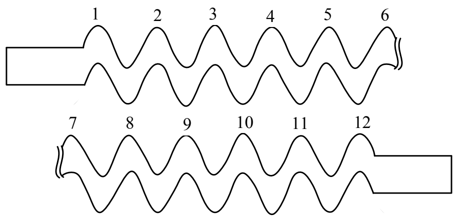	[73]	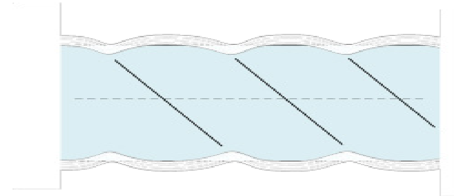
[67]	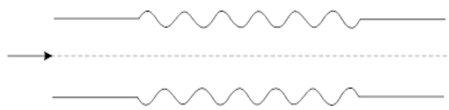	[91]	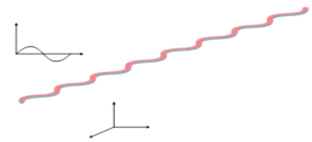
[65]	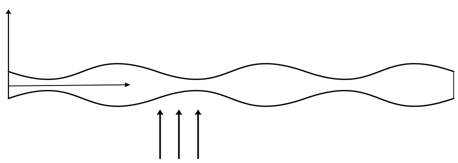	[94]	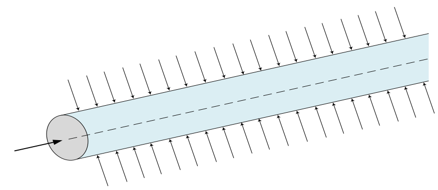
[68]	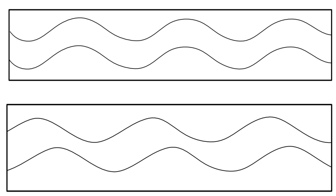	[96]	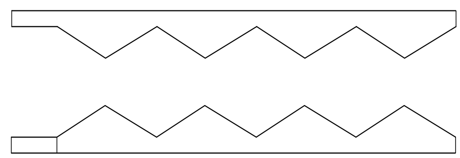
[2]	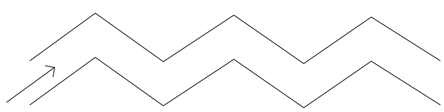	[97]	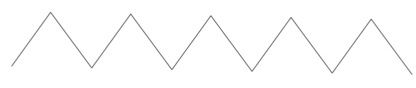
[98]	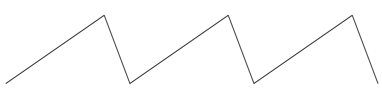	[99]	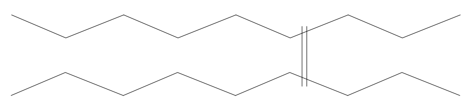
[100]	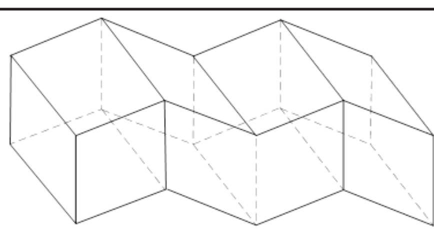	[101]	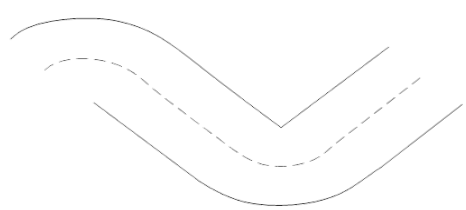

[102]	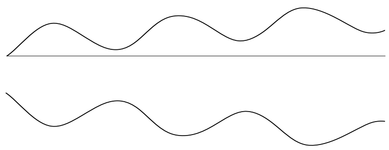	[103]	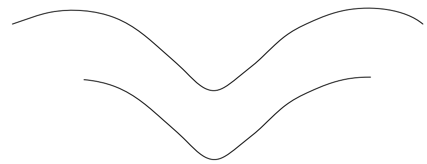
[104]	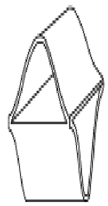	[105]	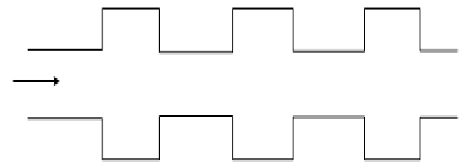
[106]	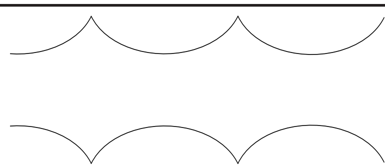	[107]	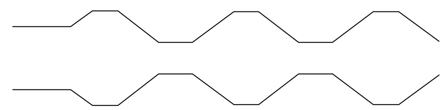
[108]	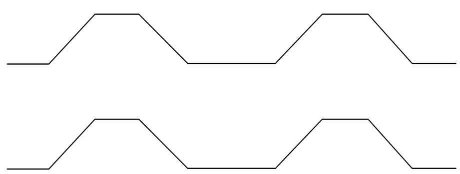	[109]	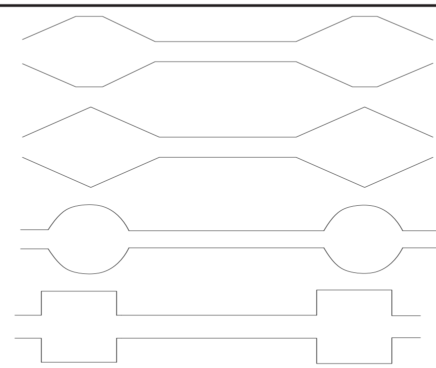

6. Uniform transient heat flux

Uniform transient heat flux refers to a time-dependent thermal boundary condition in which the heat flux applied to a surface varies with time while remaining spatially uniform across the entire heat-exchanging surface. Unlike steady-state heat flux, which remains constant, transient heat flux introduces time-dependent temperature gradients that affect the heat transfer mechanisms within the system. Mathematically, a uniform transient heat flux can be expressed as:

$$q(t) = q_m + A_q * \sin(2\pi f_q t) \tag{3}$$

where q(t) is the instantaneous heat flux (W/m²), q_m is the mean (steady) heat flux (W/m²), A_q is the amplitude of the oscillating heat flux, f_q is the frequency of oscillation (Hz), and t is the time (s).

This condition is particularly relevant in oscillatory flow heat exchangers, electronic cooling systems, regenerative heat exchangers, and thermal storage systems. The application of transient heat flux in periodic surface heat exchangers, especially when combined with oscillatory flow, is a critical factor for enhancing heat transfer. Under transient heating, the thermal boundary layer fails to reach a fully developed steady state, and thus, it undergoes periodic thinning and thickening. This continuous modulation facilitates repeated renewal of the boundary layer, maintaining high-temperature gradients along the heat exchange surface and hence increasing the Nusselt number. Furthermore, when a uniform transient heat flux is imposed on wavy surfaces under oscillatory flow, it increases secondary vortices and flow disturbances, thereby enhancing thermal diffusion and overall heat transfer efficiency. Although transient heat flux enhances heat transfer, it may influence the pressure drop in heat exchangers. An example of such an impact is increased flow resistance caused by localized thermal expansion and contraction of fluid layers adjacent to the heated surface during high-frequency transient heating. Micro-scale velocity fluctuations alter the global pressure distribution, thereby increasing flow resistance. Table 7 contains a summary of key parameters for both steady-state heat flux and uniform transient heat flux:

Table 7. Summary of key effects parameters

Parameter	Steady-State Heat Flux	Uniform Transient Heat Flux
Thermal Boundary Layer	Fully developed	Periodically regenerating
Nusselt Number (Nu)	Moderate	Higher due to enhanced convection
Secondary Flow Formation	Weak	Stronger, leading to better mixing
Pressure Drop	Standard	Can increase (5-15%) due to flow modulation

Jin et al. [110] investigated the effect of oscillatory evaporator heat loads on pressure drop oscillations (PDO) in microchannel/minichannel evaporators in the context of a pumped liquid cycle (PLC). It finds that applying an oscillatory heat load with a specific amplitude and frequency significantly reduces PDO amplitude. For instance, when a baseline heat load of 300 W is superimposed on an oscillatory component of 100 W amplitude at 6 Hz, the PDO amplitude drops by approximately 60%. Smaller amplitudes (such as 60 W) resulted in only an approximately 40% decrease, demonstrating the role of amplitude in effectiveness. Additionally, the amplitude and frequency of the PDO are stable and insensitive to high-frequency oscillations, indicating a threshold oscillation frequency of approximately 3 Hz, above which the properties of the PDO remain unchanged. Simulations were compared with a forced Van der Pol oscillator, a classical nonlinear system known for self-sustained oscillations and sensitivity to external forcing. The Van der Pol model exhibits behaviour similar to the PDO, with both systems showing comparable dynamics and trends, such as amplitude suppression at high forcing frequencies.

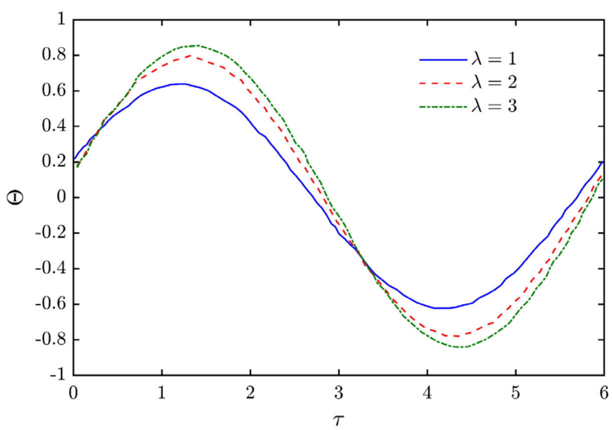

Figure 12. Transient variation of the dimensionless oscillatory heat flux(Θ)for different heat transfer parameters(λ)[111]

Khaled [111] discussed analytically the heat conduction and entropy transfer in semi-infinite and finite (slab wall) media subjected to combined periodic heat flux and convective boundary conditions. analytical solutions obtained using Laplace transform methods reveal that temperature fluctuations decrease with increasing Biot number (Bi) and decreasing heat transfer parameter (λ) and thermal oscillation parameter (P). The heat transfer parameter (λ) governs the balance between conductive and convective heat transfer mechanisms under oscillatory conditions as shown in Figure 12 [111]. This parameter is defined as:

where k is the thermal conductivity, h is the convective heat transfer coefficient, α is the thermal diffusivity, and ω is the angular frequency of the imposed heat flux.

At the surface, the amplitude of the oscillatory heat flux increases as λ rises, indicating either a smaller h or weaker convective cooling. This occurs because greater temperature variations can develop and propagate throughout the medium when convection is weaker. Therefore, one of the most important parameters for regulating the strength of thermal oscillations at the contact is λ. Ahmed and Trouv [112] investigated the transient response of biomass fuel particles to oscillatory heat flux, simulating conditions similar to those of flapping flames or varying irradiation in wildland fires. It considers radiative and convective heating for square-shaped charring (constant-volume) and non-charring (shrinking) particles with dimensions of 1 mm and 10 mmat frequencies of 0.1 and 1 Hz. The research reveals that particles generally exhibit a quasi-linear response when either irradiation or gas temperature fluctuates alone, indicating that oscillations have a minimal influence on overall particle behaviour. Yet, under combined fluctuations of gas temperature and velocity, a significant non-linear response is observed; this response enhances heat transfer, increases peak mass loss rates, and reduces burnout times by up to 70%. For example, a non-charring 1-mm particle under oscillatory convective heating (temperature amplitude 400 K, mean 700 K; velocity amplitude 1 m/s, mean 1 m/s) experienced a burnout time reduction of about 72% at both frequencies (0.1 Hz and 1 Hz), highlighting the importance of dynamic flame conditions for the proper representation of wildfire spread.

Hefny et al.[113] investigated the use of pulsating jet impingement cooling to minimize temperature fluctuations in silicon chips under transient heat-flux conditions encountered in power electronics. The performance of periodic jets with frequencies ranging from 1 to 25 Hz was investigated using numerical simulations. Results indicate that pulsating jets significantly reduce peak chip temperatures compared with steady jets, keeping peak temperatures 60°C above the inlet temperature even at a Reynolds number of 7000. A critical frequency of 19.2 Hz was identified; below this frequency, pulsating jets significantly decreased temperature oscillations. An enhancement factor (η) also indicated that pulsating jets provided improved control of temperature fluctuations, particularly at frequencies below 8.2 Hz. Additionally, intermittent jet cooling, supported by vorticity rings during off-cycles, significantly increased heat transfer coefficients (HTCs) at frequencies as low as 5 Hz. An analytical model developed for transient HTC calculations during jet off-times demonstrated accuracy, with an error of 1.5%, supporting the viability of intermittent jets as a potential thermal management scheme for future power electronics.

The effects of uniform transient heat flux have been studied in various thermal systems, including microchannels, electronics cooling, biomass combustion, and jet impingement. However, most of these studies focus on planar or straightforward geometries, primarily under unidirectional or non-oscillatory flow conditions. The interaction between oscillatory flow and uniform transient heat flux in complex geometries, such as wavy or corrugated tubes, which enhance secondary flows and boundary-layer renewal, remains poorly understood. Furthermore, the interaction between transient thermal loading and oscillation parameters (frequency, amplitude) on pressure drop behaviour, heat transfer enhancement mechanisms, and thermal boundary layer dynamics has not been thoroughly investigated. The time-resolved, nonlinear response of flow and temperature fields under genuine transient scenarios is not captured by the majority of current models, which assume idealized or constant boundary conditions. To develop predictive correlations and optimization techniques for sophisticated thermal systems, such as regenerative devices, thermoacoustic engines, and compact energy-storage exchangers, transient numerical simulations coupled with experimental validation are required. This is particularly true for oscillatory flow with a uniform, time-dependent heat flux in periodic surface heat exchangers.

7. Future research and practical recommendations

Future studies should investigate multiphase oscillatory flows, nanofluids, and AI-driven optimization techniques in addition to simplified single-phase models. These methods can reduce the cost of large-scale thermal optimization, enhance predictive accuracy, and expedite the process of identifying the optimal design parameters. Furthermore, combining topology optimisation with uncertainty quantification may yield new insights into the durability and dependability of oscillatory thermal systems under varying conditions. High-temperature operation, material durability, and dynamic control techniques should be priorities for future research aimed at real-world applications. Additionally, practical recommendations for real-world implementation can be made alongside these technical guidelines. In OPEC and other arid-region economies, hybrid oscillatory-wavy heat-exchanger arrangements should be prioritised. In hot, dry areas, implementing such systems for energy recovery and power generation could reduce water-related efficiency losses and enhance overall energy sustainability.

8. Conclusion

This paper presents an integrated evaluation of oscillatory flow behaviour in sinusoidal and corrugated geometries, focusing on its impact on the thermal and hydrodynamic performance of periodic-surface heat exchangers. The study illustrates how surface geometry and oscillatory motion interact to improve heat transfer in compact thermal systems. The uniqueness of the current review lies in its cohesive viewpoint, which surpasses previous surveys by integrating oscillatory flow and periodic surface methods under actual transient heat flux conditions. Unlike prior reviews that addressed each enhancement method separately, the present work systematically correlates oscillation parameters (frequency and amplitude) with geometric characteristics (wavelength and wave height) to highlight their synergistic effects on flow and heat transfer behaviour. These observations align with developments over the past five years, indicating that research on oscillatory flow and periodic surface designs is gradually moving from theoretical investigations to real-world engineering applications. The main findings of this review can be summarized as follows:

- Oscillatory flow significantly enhances heat transfer by inducing shear-induced mixing, vortex formation, and boundary-layer disruption.
- Improvements in heat transfer are minimal at $Re < 300$ but are substantial in turbulent and transitional regimes($Re > 2000$).
- Compared with smooth channels, sinusoidal and corrugated channel geometries can increase the Nusselt number by a factor of 4–5 through amplification of oscillatory flow effects.
- The lack of standardisation in modelling approaches and experimental setups limits direct comparisons among studies and often results in phase-lag and viscous-dissipation effects being overlooked.
- The combination of oscillation frequency, amplitude, and wavelength determines both heat transfer enhancement and pressure loss.
- In oscillating-heat-pipe, regenerative heat-exchanger, and thermoacoustic heat-exchanger systems, hybrid oscillatory–wavy configurations show significant promise for reducing pumping power and enhancing thermal efficiency.

Author contributions statement

Zina M. Salih : Writing - Original draft preparation, formal analysis, Data Collection, methodology. Saad M. Jalil: Supervision, conceptualization, Writing, Reviewing, and Editing, Methodology.

Declaration of interests

There is no conflict of interest or common interest with any institution/organization or person that may affect the review process for the paper.

Data availability

The datasets analyzed during the current study are available on request

Declaration of generative AI and AI -assisted technologies in the writing process

During the preparation of this work, the authors used Grammarly for language polishing and ChatGPT solely to improve the language and readability of the manuscript. All suggestions were carefully reviewed, revised, and verified by the authors.

Nomenclature

A, A_o	Amplitude (m)
f	Friction factor
f	Frequency, Hz
h	Heat transfer coefficient (W/m^2 K)
Nu	Nusselt number
p	Pitch (m)
P	Pressure, (Pa)
Pr	Prandtl number
q_o''	Heat flux (W/m^2)
Re	Reynold number
Re_ω	Kinetic Reynolds number
S	Axial displacement (m)
St	Strouhal number
t	Time (s)
U_o	Oscillation amplitude (m/s^2)
Wo	Womersley number
ΔZ	Tidal displacement

Greek symbols

ω	angular frequency
α	Thermal diffusivity
ω^{+}, ω^*	Dimensionless frequency
ζ_2/ζ_1	Mixing ratio
λ	Heat transfer parameter
τ_{cr}	Critical time

References

[1] P. Bouvier, P. Stouffs, and J. P. Bardon, “Experimental study of heat transfer in oscillating flow,” Int. J. Heat Mass Transf., vol. 48, no. 12, pp. 2473–2482, 2005, doi: 10.1016/j.ijheatmasstransfer.2005.01.037.

[2] S. D. Hwang, I. H. Jang, and H. H. Cho, “Experimental study on flow and local heat/mass transfer characteristics inside corrugated duct,” Int. J. Heat Fluid Flow, vol. 27, no. 1, pp. 21–32, 2006, doi: 10.1016/j.ijheatfluidflow.2005.07.001.

[3] N. Kurtulmuş and B. Sahin, “A review of hydrodynamics and heat transfer through corrugated channels,” Int. Commun. Heat Mass Transf., vol. 108, p. 104307, 2019, doi: 10.1016/j.icheatmasstransfer.2019.104307.

[4] M. N. L. Narasimhan, “Pulsating magnetohydrodynamic flow superposed on the steady laminar motion of an incompressible viscous fluid in an annular channel,” J. Phys. Soc. Japan, vol. 19, no. 1, pp. 117–120, 1964, doi: 10.1143/JPSJ.19.117.

[5] T. Okawa, T. Goto, J. Minamitani, and Y. Yamagoe, “Liquid film dryout in a boiling channel under flow oscillation conditions,” Int. J. Heat Mass Transf., vol. 52, no. 15–16, pp. 3665–3675, 2009, doi: 10.1016/j.ijheatmasstransfer.2009.02.034.

[6] D. Yin and H. B. Ma, “Analytical solution of oscillating flow in a capillary tube,” Int. J. Heat Mass Transf., vol. 66, pp. 699–705, 2013, doi: 10.1016/j.ijheatmasstransfer.2013.07.073.

[7] C. Xu, S. Xu, Z. Wang, and D. Fenga, “Experimental investigation of flow and heat transfer characteristics of pulsating flows driven by wave signals in a microchannel heat sink,” Int. Commun. Heat Mass Transf., vol. 125, p. 105343, 2021, doi: 10.1016/j.icheatmasstransfer.2021.105343.

[8] C. Wantha, “Effect and heat transfer correlations of finned tube heat exchanger under unsteady pulsating flows,” Int. J. Heat Mass Transf., vol. 99, pp. 141–148, 2016, doi: 10.1016/j.ijheatmasstransfer.2016.03.102.

[9] Y. Liu, J. Lei, B. Wang, X. Deng, D. Sun, and H. Wang, “Experimental and simulation study on oscillating flow and heat transfer characteristics of the cooling gallery in steel pistons,” Case Stud. Therm. Eng., vol. 58, no. April, p. 104436, 2024, doi: 10.1016/j.csite.2024.104436.

[10] R. Pendyala, S. Jayanti, and A. R. Balakrishnan, “Convective heat transfer in single-phase flow in a vertical tube subjected to axial low frequency oscillations,” Heat Mass Transf. und Stoffuebertragung, vol. 44, no. 7, pp. 857–864, 2008, doi: 10.1007/s00231-007-0302-3.

[11] J. D. Patil and B. S. Gawali, “Experimental study of heat transfer characteristics in oscillating fluid flow in tube,” Exp. Heat Transf., vol. 30, no. 4, pp. 328–340, 2017, doi: 10.1080/08916152.2016.1258018.

[12] S. M. Jalil, “Mathematical and numerical predictions for optimum perfect mixing by bulk convective oscillatory exchange,” Int. J. Heat Mass Transf., vol. 167, p. 120792, 2021, doi: 10.1016/j.ijheatmasstransfer.2020.120792.

[13] J. Liu, G. Xie, and B. Sundén, “Flow pattern and heat transfer past two tandem arranged cylinders with oscillating inlet velocity,” Appl. Therm. Eng., vol. 120, pp. 614–625, Jun. 2017, doi: 10.1016/j.applthermaleng.2017.04.032.

[14] W. Kamsanam, X. Mao, and A. J. Jaworski, “Thermal performance of finned-tube thermoacoustic heat exchangers in oscillatory flow conditions,” Int. J. Therm. Sci., vol. 101, pp. 169–180, 2016, doi: 10.1016/j.ijthermalsci.2015.10.032.

[15] S. M. Jalil, “Numerical characterization of viscous heat dissipation rate in oscillatory air flow,” J. Heat Transfer, vol. 142, no. 1, 2020, doi: 10.1115/1.4045173.

[16] S. M. Jalil, “Experimental and numerical investigation of axial heat transfer enhancement by oscillatory flows,” p. 373426, 2019.

[17] G. J. Brereton and S. M. Jalil, “Diffusive heat and mass transfer in oscillatory pipe flow,” Phys. Fluids, vol. 29, no. 7, 2017, doi: 10.1063/1.4990976.

[18] G. J. B. · S. M. J. · S. K. · J. M. S. Year:, “Axial heat-transfer enhancement by flow oscillation for high heat-flux applications,” no. March, p. 2022, 2022.

[19] G. J. Brereton and S. M. Jalil, “Axial conduction and dissipation in oscillatory laminar pipe flow at low and high frequencies,” Phys. Fluids, vol. 31, no. 8, 2019, doi: 10.1063/1.5093328.

[20] U. Akdag and A. F. Ozguc, “Experimental investigation of heat transfer in oscillating annular flow,” Int. J. Heat Mass Transf., vol. 52, no. 11–12, pp. 2667–2672, 2009, doi: 10.1016/j.ijheatmasstransfer.2009.01.006.

[21] U. Akdag, M. Ozdemir, and A. F. Ozguc, "Heat removal from oscillating flow in a vertical annular channel," Heat Mass Transf. und Stoffuebertragung, vol. 44, no. 4, pp. 393–400, 2008, doi: 10.1007/s00231-007-0248-5.

[22] B. S. Gawali, "Experimental investigation of heat transfer enhancement factors in the oscillating flow heat exchanger using Kurzweg's and Nishio's correlations," Exp. Therm. Fluid Sci., vol. 83, pp. 37–46, 2017, doi: 10.1016/j.expthermflusci.2016.12.014.

[23] K. Tang, J. Yu, T. Jin, Y. P. Wang, W. T. Tang, and Z. H. Gan, "Heat transfer of laminar oscillating flow in finned heat exchanger of pulse tube refrigerator," Int. J. Heat Mass Transf., vol. 70, pp. 811–818, 2014, doi: 10.1016/j.ijheatmasstransfer.2013.11.067.

[24] W. Z. Xiangyu Luo, Weichen Zhang, Haitao Dong, Amrit Kumar Thakur, Bing Yang, "Numerical analysis of heat transfer enhancement of fluid past an oscillating circular cylinder in laminar flow regime," vol. 3, no. 5, p. 6, 2021.

[25] S. M. Jalil, "Phase-lags' radial variations between velocity, shear stress, and pressure gradient in ultrahigh frequency pulsating turbulent flows," J. Fluids Eng. Trans. ASME, vol. 142, no. 5, pp. 1–14, 2020, doi: 10.1115/1.4045570.

[26] L. Shemer, I. Wygnanski, and E. Kit, "Pulsating flow in a pipe," J. Fluid Mech., vol. 153, pp. 313–337, 1985, doi: 10.1017/S0022112085001276.

[27] R. R. Mankbadi and J. T. C. Liu, "Near-wall response in turbulent shear flows subjected to imposed unsteadiness," J. Fluid Mech., vol. 238, no. 55, pp. 55–71, 1992, doi: 10.1017/S0022112092001630.

[28] K. Rosenberg et al., "Phase relationships between velocity, wall pressure, and wall shear stress in a forced turbulent boundary layer," 46th AIAA Fluid Dyn. Conf., no. June, pp. 1–7, 2016, doi: 10.2514/6.2016-4396.

[29] G. J. Brereton and R. R. Mankbadi, "A Rapid-Distortion-Theory Turbulence Model for Developed Unsteady Wall-Bounded Flow," NASA Tech. Memo., no. July, 1993.

[30] A. A. Mishra and S. S. Girimaji, "Toward approximating non-local dynamics in single-point pressure-strain correlation closures," J. Fluid Mech., vol. 811, pp. 168–188, 2017, doi: 10.1017/jfm.2016.730.

[31] G. Binder, S. Tardu, R. F. Blackwelder, and J. L. Kueny, "Large Amplitude Periodic Oscillations in the Wall Region of a Turbulent Channel Flow.," 1985.

[32] D. Ronneberger, "Investigation of the Dynamics of a Turbulent Wall Boundary Layer By Introduction of a Small External Perturbation.," p. 30201, 1985.

[33] S. He and J. D. Jackson, "An experimental study of pulsating turbulent flow in a pipe," Eur. J. Mech. B/Fluids, vol. 28, no. 2, pp. 309–320, 2009, doi: 10.1016/j.euromechflu.2008.05.004.

[34] L. R. J. Sundstrom and M. J. Cervantes, "Characteristics of the wall shear stress in pulsating wall-bounded turbulent flows," Exp. Therm. Fluid Sci., vol. 96, pp. 257–265, 2018, doi: 10.1016/j.expthermflusci.2018.02.036.

[35] P. K. Papadopoulos and A. P. Vouros, "Pulsating turbulent pipe flow in the current dominated regime at high and very-high frequencies," Int. J. Heat Fluid Flow, vol. 58, pp. 54–67, 2016, doi: 10.1016/j.ijheatfluidflow.2015.12.007.

[36] G. J. B. · S. M. J. · S. K. · J. M.Slike, "Axial heat-transfer enhancement by low oscillation for high heat-flux.pdf."

[37] R. Blythman, T. Persoons, N. Jeffers, and D. B. Murray, "Effect of oscillation frequency on wall shear stress and pressure drop in a rectangular channel for heat transfer applications," J. Phys. Conf. Ser., vol. 745, no. 3, 2016, doi: 10.1088/1742-6596/745/3/032044.

[38] H. Yuan, S. Tan, J. Wen, and N. Zhuang, "Heat transfer of pulsating laminar flow in pipes with wall thermal inertia," Int. J. Therm. Sci., vol. 99, pp. 152–160, 2016, doi: 10.1016/j.ijthermalsci.2015.08.014.

[39] D. Yin and H. B. Ma, "Analytical solution of heat transfer of oscillating flow at a triangular pressure waveform," Int. J. Heat Mass Transf., vol. 70, pp. 46–53, 2014, doi: 10.1016/j.ijheatmasstransfer.2013.10.016.

[40] E. J. Watson, "Diffusion in oscillatory pipe flow," J. Fluid Mech., vol. 133, pp. 233–244, 1983, doi: 10.1017/S0022112083001883.

[41] W. Kamsanam, X. Mao, and A. J. Jaworski, "Development of experimental techniques for measurement of heat transfer rates in heat exchangers in oscillatory flows," Exp. Therm. Fluid Sci., vol. 62, pp. 202–215, 2015, doi: 10.1016/j.expthermflusci.2014.12.008.

[42] A. S. Slutsky and R. D. Kamm, "An experimental study of gas exchange in laminar oscillatory flow," J. Fluid Mech., vol. 133, no. HY8, pp. 245–254, 1983, doi: 10.1017/S0022112083001895.

[43] Q. Dai, Y. Chen, and L. Yang, "CFD investigation on characteristics of oscillating flow and heat transfer in 3D pulse tube," Int. J. Heat Mass Transf., vol. 84, pp. 401–408, 2015, doi: 10.1016/j.ijheatmasstransfer.2015.01.027.

[44] J. C. U. and A. M. Ali J. Chamkha, "Oscillatory Flow and Heat Transfer in Two Immiscible Fluids," vol. 31, no. 1, pp. 1–3, 2004.

[45] X. Shi and J. M. Khodadadi, "Periodic state of fluid flow and heat transfer in a lid-driven cavity due to an oscillating thin fin," 2005. doi: 10.1016/j.ijheatmasstransfer.2005.07.026.

[46] A. V. Krishna, A. Varma, and K. Nidhul, "Heat transfer and entropy generation characteristics of nanofluid flow over bluff bodies under steady and unsteady flow: A two-phase approach," Case Stud. Therm. Eng., vol. 63, no. July, p. 105242, 2024, doi: 10.1016/j.csite.2024.105242.

[47] H. Gomaa and A. M. Al Taweel, "Effect of oscillatory motion on heat transfer at vertical flat surfaces," 2005. doi: 10.1016/j.ijheatmasstransfer.2004.10.017.

[48] D. W. Zhao, G. H. Su, Z. H. Liang, Y. J. Zhang, W. X. Tian, and S. Z. Qiu, "Experimental research on transient critical heat flux in vertical tube under oscillatory flow condition," Int. J. Multiph. Flow, vol. 37, no. 9, pp. 1235–1244, 2011, doi: 10.1016/j.ijmultiphaseflow.2011.06.012.

[49] K. Zhang, Y. J. Huang, H. B. You, W. X. Tian, G. H. Su, and S. Z. Qiu, "Experimental investigations on single-phase convection and critical heat flux in vertical tubes under oscillatory flow condition," Ann. Nucl. Energy, vol. 143, 2020, doi: 10.1016/j.anucene.2020.107433.

[50] R. Siegel and M. Perlmutter, "Laminar heat transfer in a channel with unsteady flow and wall heating varying with position and time," J. Heat Transfer, vol. 85, no. 4, pp. 358–365, 1963, doi: 10.1115/1.3686125.

[51] M. Hadžiabdić, E. Palkin, R. Mullyadzhanov, and K. Hanjalić, "Heat transfer in flow around a rotary oscillating cylinder at a high subcritical Reynolds number: A computational study," Int. J. Heat Fluid Flow, vol. 79, no. July, p. 108441, 2019, doi: 10.1016/j.ijheatfluidflow.2019.108441.

[52] W. S. Fu and B. H. Tong, "Numerical investigation of heat transfer from a heated oscillating cylinder in cross flow," Int. J. Heat Mass Transf., vol. 45, no. 14, pp. 3033–3043, 2002, doi: 10.1016/S0017-9310(02)00016-9.

[53] U. Akdag, S. Akcay, and D. Demiral, "Heat transfer enhancement with laminar pulsating nanofluid flow in a wavy channel," Int. Commun. Heat Mass Transf., vol. 59, pp. 17–23, 2014, doi: 10.1016/j.icheatmasstransfer.2014.10.008.

[54] A. Korichi and L. Oufer, "Heat transfer enhancement in oscillatory flow in channel with periodically upper and lower walls mounted obstacles," Int. J. Heat Fluid Flow, vol. 28, no. 5, pp. 1003–1012, 2007, doi: 10.1016/j.ijheatfluidflow.2006.11.002.

[55] Y. Li, Q. Yu, S. Yu, B. Gong, and J. Zhang, "Numerical investigation of pulsating flow structures and heat transfer enhancement performance in spherical corrugated helical tube," Appl. Therm. Eng., vol. 213, pp. 1–23, 2022, doi: 10.1016/j.applthermaleng.2022.118647.

[56] F. Xin, Z. Liu, N. Zheng, P. Liu, and W. Liu, "Numerical study on flow characteristics and heat transfer enhancement of oscillatory flow in a spirally corrugated tube," Int. J. Heat Mass Transf., vol. 127, pp. 402–413, 2018, doi: 10.1016/j.ijheatmasstransfer.2018.06.139.

[57] L. Zhang et al., "Study of the enhanced heat transfer characteristics of wavy-walled tube heat exchangers under pulsating flow fields," Phys. Fluids, vol. 35, no. 11, pp. 1–21, 2023, doi: 10.1063/5.0173932.

[58] G. Russ and H. Beer, "Heat transfer and flow field in a pipe with sinusoidal wavy surface - I. Numerical investigation," Int. J. Heat Mass Transf., vol. 40, no. 5, pp. 1061–1070, 1997, doi: 10.1016/0017-9310(96)00158-5.

[59] G. Russ and H. Beer, "Heat transfer and flow field in a pipe with sinusoidal wavy surface - II. Experimental investigation," Int. J. Heat Mass Transf., vol. 40, no. 5, pp. 1071–1081, 1997, doi: 10.1016/0017-9310(96)00159-7.

[60] J. H. Jang and W. M. Yan, "Mixed convection heat and mass transfer along a vertical wavy surface," Int. J. Heat Mass Transf., vol. 47, no. 3, pp. 419–428, 2004, doi: 10.1016/j.ijheatmasstransfer.2003.07.020.

[61] S. Harikrishnan and S. Tiwari, "Effect of skewness on flow and heat transfer characteristics of a wavy channel," Int. J. Heat Mass Transf., vol. 120, pp. 956–969, 2018, doi: 10.1016/j.ijheatmasstransfer.2017.12.120.

[62] A. G. Ramgadia and A. K. Saha, "Fully developed flow and heat transfer characteristics in a wavy passage: Effect of amplitude of waviness and Reynolds number," Int. J. Heat Mass Transf., vol. 55, no. 9–10, pp. 2494–2509, 2012, doi: 10.1016/j.ijheatmasstransfer.2012.01.010.

[63] S. W. Chang, A. W. Lees, and T. C. Chou, "Heat transfer and pressure drop in furrowed channels with transverse and skewed sinusoidal wavy walls," Int. J. Heat Mass Transf., vol. 52, no. 19–20, pp. 4592–4603, 2009, doi: 10.1016/j.ijheatmasstransfer.2009.02.039.

[64] A. M. Guzmán, M. J. Cárdenas, F. A. Urzúa, and P. E. Araya, "Heat transfer enhancement by flow bifurcations in asymmetric wavy wall channels," Int. J. Heat Mass Transf., vol. 52, no. 15–16, pp. 3778–3789, 2009, doi: 10.1016/j.ijheatmasstransfer.2009.02.026.

[65] H. Bai, Z. Lin, M. M. Alam, and F. Zhao, "Near wake flow and forced convection heat transfer of sinusoidal wavy cylinder based on flow decomposition," Int. J. Heat Mass Transf., vol. 202, 2023, doi: 10.1016/j.ijheatmasstransfer.2022.123753.

[66] Y. G. Lv, Z. X. Wen, Q. Li, and Y. Qiu, "Numerical investigation on thermal hydraulic performance of hybrid wavy channels in a supercritical CO2 precooler," Int. J. Heat Mass Transf., vol. 181, 2021, doi: 10.1016/j.ijheatmasstransfer.2021.121891.

[67] M. A. Ahmed, N. H. Shuaib, and M. Z. Yusoff, "Numerical investigations on the heat transfer enhancement in a wavy channel using nanofluid," Int. J. Heat Mass Transf., vol. 55, no. 21–22, pp. 5891–5898, 2012, doi: 10.1016/j.ijheatmasstransfer.2012.05.086.

[68] A. Ahmadpour and S. M. A. Noori Rahim Abadi, "Thermal-hydraulic performance evaluation of gas-liquid multiphase flows in a vertical sinusoidal wavy channel in the presence/absence of phase change," Int. J. Heat Mass Transf., vol. 138, pp. 677–689, 2019, doi: 10.1016/j.ijheatmasstransfer.2019.04.084.

[69] R. Daba, S. Xu, W. Wang, Y. Huang, X. Luo, and K. Fang, "Effect of flow pulsation on heat transfer performance of biomimetic bark microchannel heat sink," Case Stud. Therm. Eng., vol. 56, no. March, p. 104255, 2024, doi: 10.1016/j.csite.2024.104255.

[70] T. K. Nguyen et al., "Influence of various shapes of CuO nanomaterial on nanofluid forced convection within a sinusoidal channel with obstacles," Chem. Eng. Res. Des., vol. 146, pp. 478–485, 2019, doi: 10.1016/j.cherd.2019.04.030.

[71] S. Valiallah Mousavi, M. B. Gerdroodbary, M. Sheikholeslami, and D. D. Ganji, "The influence of a magnetic field on the heat transfer of a magnetic nanofluid in a sinusoidal channel," Eur. Phys. J. Plus, vol. 131, no. 9, 2016, doi: 10.1140/epjp/i2016-16347-4.

[72] M. Sun and M. Zeng, "Investigation on turbulent flow and heat transfer characteristics and technical economy of corrugated tube," Appl. Therm. Eng., vol. 129, pp. 1–11, 2018, doi: 10.1016/j.applthermaleng.2017.09.136.

[73] F. Andrade, A. S. Moita, A. Nikulin, A. L. N. Moreira, and H. Santos, "Experimental investigation on heat transfer and pressure drop of internal flow in corrugated tubes," Int. J. Heat Mass Transf., vol. 140, pp. 940–955, 2019, doi: 10.1016/j.ijheatmasstransfer.2019.06.025.

[74] M. Bayareh and A. Nourbakhsh, "Numerical Simulation and Analysis of Heat Transfer for Different Geometries of Corrugated Tubes in a Double Pipe Heat Exchanger," J. Therm. Eng., vol. 5, no. 4, pp. 293–301, 2019, doi: 10.18186/THERMAL.581775.

[75] A. S. Varkaneh, G. A. S. Nooshabadi, and A. A. A. Arani, "Flow field and heat transfer of ferromagnetic nanofluid in presence of magnetic field inside a corrugated tube," J. Therm. Eng., vol. 9, no. 5, pp. 1667–1686, 2023, doi: 10.18186/THERMAL.1401685.

[76] A. R. Al-Obaidi, "Investigation of fluid field analysis, characteristics of pressure drop and improvement of heat transfer in three-dimensional circular corrugated pipes," J. Energy Storage, vol. 26, no. October, 2019, doi: 10.1016/j.est.2019.101012.

[77] J. I. Córcoles, J. D. Moya-Rico, A. E. Molina, and J. A. Almendros-Ibáñez, "Numerical and experimental study of the heat transfer process in a double pipe heat exchanger with inner corrugated tubes," Int. J. Therm. Sci., vol. 158, no. May, 2020, doi: 10.1016/j.ijthermalsci.2020.106526.

[78] V. I. Artemov, K. B. Minko, and G. G. Yan'kov, "Numerical simulation of fluid flow in an annular channel with outer transversally corrugated wall," Int. J. Heat Mass Transf., vol. 90, pp. 743–751, 2015, doi: 10.1016/j.ijheatmasstransfer.2015.07.020.

[79] G. Wang and S. P. Vanka, "Convective heat transfer in periodic wavy passages," Int. J. Heat Mass Transf., vol. 38, no. 17, pp. 3219–3230, 1995, doi: 10.1016/0017-9310(95)00051-A.

[80] B. Ničeno and E. Nobile, "Numerical analysis of fluid flow and heat transfer in periodic wavy channels," Int. J. Heat Fluid Flow, vol. 22, no. 2, pp. 156–167, 2001, doi: 10.1016/S0142-727X(01)00074-1.

[81] H. M. S. Bahaidarah, "A numerical study of fluid flow and heat transfer characteristics in channels with staggered wavy walls," Numer. Heat Transf. Part A Appl., vol. 51, no. 9, pp. 877–898, 2007, doi: 10.1080/10407780600939644.

[82] H. M. Metwally and R. M. Manglik, "Enhanced heat transfer due to curvature-induced lateral vortices in laminar flows in sinusoidal corrugated-plate channels," Int. J. Heat Mass Transf., vol. 47, no. 10–11, pp. 2283–2292, 2004, doi: 10.1016/j.ijheatmasstransfer.2003.11.019.

[83] Y. Sui, C. J. Teo, and P. S. Lee, "Direct numerical simulation of fluid flow and heat transfer in periodic wavy channels with rectangular cross-sections," Int. J. Heat Mass Transf., vol. 55, no. 1–3, pp. 73–88, 2012, doi: 10.1016/j.ijheatmasstransfer.2011.08.041.

[84] M. Sarkar, S. B. Paramane, and A. Sharma, "Periodically Fully Developed Heat and Fluid Flow Characteristics in a Furrowed Wavy Channel," Heat Transf. Eng., vol. 38, no. 2, pp. 278–288, 2017, doi: 10.1080/01457632.2016.1177434.

[85] M. Z. Hossain and A. K. M. S. Islam, "Fully developed flow structures and heat transfer in sine-shaped wavy channels," 2004. doi: 10.1016/S0735-1933(04)00075-2.

[86] T. D. Manh, M. Bahramkhoo, M. Barzegar Gerdroodbary, N. D. Nam, and I. Tlili, "Investigation of nanomaterial flow through non-parallel plates," J. Therm. Anal. Calorim., vol. 143, no. 5, pp. 3867–3875, 2021, doi: 10.1007/s10973-020-09352-0.

[87] T. D. Manh, A. M. Abazari, M. Barzegar Gerdroodbary, N. D. Nam, R. Moradi, and H. Babazadeh, "Computational simulation of variable magnetic force on heat characteristics of backward-facing step flow," J. Therm. Anal. Calorim., vol. 144, no. 4, pp. 1585–1596, 2021, doi: 10.1007/s10973-020-09608-9.

[88] M. Barzegar Gerdroodbary, M. Jafaryar, M. Sheikholeslami, and Y. Amini, "The efficacy of magnetic force on thermal performance of ferrofluid in a screw tube," Case Stud. Therm. Eng., vol. 49, no. June, p. 103187, 2023, doi: 10.1016/j.csite.2023.103187.

[89] S. Mosayebidorcheh and M. Hatami, "Analytical investigation of peristaltic nanofluid flow and heat transfer in an asymmetric wavy wall channel (Part I: Straight channel)," Int. J. Heat Mass Transf., vol. 126, pp. 790–799, 2018, doi: 10.1016/j.ijheatmasstransfer.2018.05.080.

[90] H. S. Yoon, S. H. Nam, and M. Il Kim, "Laminar forced convection heat transfer around wavy elliptic cylinders with different aspect ratios," Int. J. Heat Mass Transf., vol. 194, 2022, doi: 10.1016/j.ijheatmasstransfer.2022.123038.

[91] Z. X. Wen, J. L. Wu, S. S. Wang, J. Q. Cheng, and Q. Li, "Numerical study and machine learning on local flow and heat transfer characteristics of supercritical carbon dioxide mixtures in a sinusoidal wavy channel PCHE," Int. J. Heat Mass Transf., vol. 223, no. February, 2024, doi: 10.1016/j.ijheatmasstransfer.2024.125278.

[92] L. Zhang et al., "Analysis of nanofluid flow and heat transfer characteristics in a wavy-walled tube heat exchanger," Int. J. Heat Fluid Flow, vol. 108, no. June, 2024, doi: 10.1016/j.ijheatfluidflow.2024.109488.

[93] L. Zhang et al., "Heat transfer and flow characteristics of fluids in wavy-walled tubes under the combined effect of vibrations and pulsations," Appl. Therm. Eng., vol. 268, no. December 2024, 2025, doi: 10.1016/j.applthermaleng.2025.125853.

[94] A. R. Al-Obaidi and J. Alhamid, "Investigation of flow pattern, thermohydraulic performance and heat transfer improvement in 3D corrugated circular pipe under varying structure configuration parameters with development different correlations," Int. Commun. Heat Mass Transf., vol. 126, no. June, 2021, doi: 10.1016/j.icheatmasstransfer.2021.105394.

[95] T. Nishimura and N. Kojima, "Mass transfer enhancement in a symmetric sinusoidal wavy-walled channel for pulsatile flow," Int. J. Heat Mass Transf., vol. 38, no. 9, pp. 1719–1731, 1995, doi: 10.1016/0017-9310(94)00275-Z.

[96] P. Naphon, "Heat transfer characteristics and pressure drop in channel with V corrugated upper and lower plates," Energy Convers. Manag., vol. 48, no. 5, pp. 1516–1524, 2007, doi: 10.1016/j.enconman.2006.11.020.

[97] Y. Islamoglu and A. Kurt, "Heat transfer analysis using ANNs with experimental data for air flowing in corrugated channels," Int. J. Heat Mass Transf., vol. 47, no. 6–7, pp. 1361–1365, 2004, doi: 10.1016/j.ijheatmasstransfer.2003.07.031.

[98] Y. Islamoglu and C. Parmaksizoglu, "Numerical investigation of convective heat transfer and pressure drop in a corrugated heat exchanger channel," Appl. Therm. Eng., vol. 24, no. 1, pp. 141–147, 2004, doi: 10.1016/j.applthermaleng.2003.07.004.

[99] M. Sakr, "Convective heat transfer and pressure drop in V-corrugated channel with different phase shifts," Heat Mass Transf. und Stoffuebertragung, vol. 51, no. 1, pp. 129–141, 2015, doi: 10.1007/s00231-014-1390-5.

[100] P. Taylor, "Numerical Heat Transfer , Part A : Applications : An International Journal of Computation and Methodology EFFECT OF ASPECT RATIO ON CONVECTION ENHANCEMENT IN WAVY CHANNELS," no. October 2014, pp. 37–41, doi: 10.1080/713838173.

[101] Z. Zheng, D. F. Fletcher, and B. S. Haynes, "International Journal of Heat and Mass Transfer Transient laminar heat transfer simulations in periodic zigzag channels," Int. J. Heat Mass Transf., vol. 71, pp. 758–768, 2014, doi: 10.1016/j.ijheatmasstransfer.2013.12.056.

[102] F. Oviedo-tolentino, R. Romero-méndez, and A. Hernández-guerrero, "Use of diverging or converging arrangement of plates for the control of chaotic mixing in symmetric sinusoidal plate channels," Exp. Therm. Fluid Sci., vol. 33, no. 2, pp. 208–214, 2009, doi: 10.1016/j.expthermflusci.2008.08.002.

[103] M. Gradeck, B. Hoareau, and M. Lebouche, "Local analysis of heat transfer inside corrugated channel ´," vol. 48, pp. 1909–1915, 2005, doi: 10.1016/j.ijheatmasstransfer.2004.12.026.

[104] M. Ciofalo and J. Stasiek, "Investigation corrugated of flow and heat transfer Numerical simulations," vol. 39, no. 1, 1995.

[105] N. Tokgoz, M. M. Aksoy, and B. Sahin, "Investigation of flow characteristics and heat transfer enhancement of corrugated duct geometries," Appl. Therm. Eng., vol. 118, pp. 518–530, 2017, doi: 10.1016/j.applthermaleng.2017.03.013.

[106] N. Paisarn, "Study on the heat-transfer characteristics and pressure drop in channels with arc-shaped wavy plates," J. Eng. Phys. Thermophys., vol. 83, no. 5, pp. 1061–1069, 2010, doi: 10.1007/s10891-010-0431-2.

[107] M. A. Ahmed, M. Z. Yusoff, and N. H. Shuaib, "Effects of geometrical parameters on the flow and heat transfer characteristics in trapezoidal-corrugated channel using nanofluid," Int. Commun. Heat Mass Transf., vol. 42, pp. 69–74, 2013, doi: 10.1016/j.icheatmasstransfer.2012.12.012.

[108] A. M. Abed, M. A. Alghoul, K. Sopian, H. A. Mohammed, H. sh Majdi, and A. N. Al-Shamani, "Design characteristics of corrugated trapezoidal plate heat exchangers using nanofluids," Chem. Eng. Process. Process Intensif., vol. 87, pp. 88–103, 2015, doi: 10.1016/j.cep.2014.11.005.

[109] A. A. Ramadhan, Y. T. Al Anii, and A. J. Shareef, "Groove geometry effects on turbulent heat transfer and fluid flow," Heat Mass Transf. und Stoffuebertragung, vol. 49, no. 2, pp. 185–195, 2013, doi: 10.1007/s00231-012-1076-9.

[110] Q. Jin, J. T. Wen, and S. Narayan, "Effect of Oscillatory Heat Load on Pressure Drop Oscillation," Int. J. Heat Mass Transf., vol. 194, p. 123077, 2022, doi: 10.1016/j.ijheatmasstransfer.2022.123077.

[111] A. R. A. Khaled, "Conduction heat and entropy transfer in a semi-infinite medium and wall with a combined periodic heat flux and convective boundary condition," Int. J. Therm. Sci., vol. 47, no. 1, pp. 76–83, 2008, doi: 10.1016/j.ijthermalsci.2007.01.011.

[112] M. M. Ahmed and A. Trouvé, "Simulations of the unsteady response of biomass burning particles exposed to oscillatory heat flux conditions," Fire Saf. J., vol. 120, no. January 2020, 2021, doi: 10.1016/j.firesaf.2020.103059.

[113] M. Hefny, J. S. Cotton, and A. Emadi, "The use of pulsating jet impingement to minimize temperature oscillations caused by fluctuating heat-flux boundary conditions," Appl. Therm. Eng., vol. 258, no. September 2024, 2025, doi: 10.1016/j.applthermaleng.2024.124650.